Title
SOME PHYSICAL CONSEQUENCES OF THE ABFST MULTIPERIPHERAL MODEL

Author
Chan, Chun-Fai.

Publication Date
1972-08-01

LBL-1038

SOME PHYSICAL CONSEQUENCES OF THE ABFST MULTIPERIPHERAL MODEL

Chun-Fai Chan
(Ph. D. Thesis)

August 14, 1972

AEC Contract No. W-7405-eng-48

DISCLAIMER

SOME PHYSICAL CONSEQUENCES OF THE ABFST MULTIPERIPHERAL MODEL*

Chun-Fai Chan

Lawrence Berkeley Laboratory
University of California
Berkeley, California 94720

August 14, 1972

ABSTRACT

The solution of the Amati-Bertocchi-Fubini-Stanghellini-Tonin multiperipheral integral equation with a narrow-resonance kernel is investigated. First, an approximate scheme that leads to a tractable analytic approximate solution is presented for both the forward and nonforward equations. Next, the exact numerical solutions are displayed for the relevant values of the input parameters: These results serve as a measure of the accuracy of various analytic approximate solutions. The approximate solution present here is found to be good to within about 10% in the region of interest. The absolute magnitude of the high energy pseudoscalar-meson (μ) - baryon (B) total cross section is calculated in an SU(3)- symmetric model by using this approximate solution and the approximation that the low energy μB amplitude is dominated by the baryon pole plus the first elastic resonance. The result is comparable to data at the presently highest available energy. The theoretical and phenomenological implications of the high energy off-shell behavior given by this solution are also studied. The improvement of the model by including the high energy scattering part in the kernel, thus giving a new solution consisting of Regge pole and cut, is briefly discussed.

I. INTRODUCTION

In this paper we shall study high energy hadron-hadron scattering with the ABFST multiperipheral model.[1-3] The input to the problem will be mainly the knowledge of the interaction at low energy, i.e., around 1 GeV^2. By this we mean that, in the relation of the cross sections

$$\sigma^{tot} = \sigma^{el} + \sum_n \sigma^n , \tag{1.1}$$

we assume σ^n involves mainly the formation of (two-body) resonances in each unit block of the multiperipheral chain. Correspondingly, in the integral equation

$$\sigma^{tot} = \sigma^{el} + \int \sigma^{el} S \, \sigma^{tot} , \tag{1.2}$$

we assume the kernel $K = \sigma^{el} S$ (where S is the metric in the integration) consists mainly of the resonance part of σ^{el}. Each σ^n will then have the characteristic of rapid rising and falling behavior as a function of the energy s. We believe it is mainly the sum of these "peaks" that gives rise to the observed magnitude of σ^{tot}. Such a composition is justified to some extent by the existing data, for example, in the data of K^+N scattering.[4] Due to exchange degeneracy of the secondary j-plane singularities, in this case we have exclusively (or almost) diffractive scattering for $\sigma^{tot}_{K^+N}$. A portion of the composition is sketched in Fig. 1.

In a more serious approach, as pointed out in Ref. 2, we should include the high energy scattering part in σ^n, and correspondingly the high energy scattering part in the kernel $K = \sigma^{el} S$ as well. This gives each σ^n a small but constant (or almost constant)

tail. And there comes the question of self-consistency in the high energy scattering parts in the output σ^{tot} and the input σ^{el}.

(We remark that this picture seems in contradiction with the self-bootstrapping Pomeranchukon model in which each σ^n has only a constant part due to the diffractive production process in itself.)

We shall first investigate in Sec. II the solution of the multiperipheral integral equation with a resonance kernel only, and then study in Secs. III and IV some physical consequences of this solution. The question of including the high energy tail in the kernel will be discussed briefly in Sec. V.

II. SOLUTION OF THE ABFST EQUATION WITH A RESONANCE KERNEL

A. Preface

In this section we shall investigate in two complementary ways the solution of the ABFST multiperipheral integral equation,[1] in the modern version formulated by Chew, Rogers, and Snider,[2] and by Abarbanel, Chew, Goldberger, and Saunders.[3] We shall study in detail the solution of the equation with the simplest kernel consisting of a single sharp resonance, and discuss only briefly the straightforward generalization to the case of a kernel with many resonances. This solution, in the language of Ref. 3, corresponds to the "unperturbed solution," since we neglect the small high-subenergy diffractive scattering part in the input kernel.

In order to gain insight into the nature of the output, we first obtain an analytic approximate solution by replacing the original kernel by a factorizable kernel. This replacement is guided in some sense by "peripheralism," that is, the factorizable kernel should behave like the original kernel in the peripheral region, where the contribution to any convergent integral involved is expected to be important. We shall demonstrate that the solution so obtained reproduces itself under the action of the original kernel in the most peripheral region.

On the other hand, we have also solved the equation numerically for certain values of the input parameters. This solution provides a measure of the accuracy of various analytic approximate solutions.

Our analytic approximate method is presented in subsection B (for forward scattering) and subsection C (for nonforward scattering). There is no pretense of rigor; rather, in a practical way we shall develop a tractable explicit form that is simple enough and yet has

reasonable accuracy. The latter point is justified by comparing with the exact numerical solution which is presented in subsection D. Some generalizations and the question of the uniqueness of our approximation scheme are presented at the end of this section.

B. THE FORWARD EQUATION AND THE APPROXIMATE SOLUTION

We shall first illustrate the properties of our approximation in the case of forward scattering ($q = 0$ in Fig. 2). Let us here ignore the problem of internal symmetry; this can easily be incorporated into the model by introducing crossing matrices as described in Sec. III. The absorptive part A of the elastic amplitude T of pseudoscalar-meson—pseudoscalar-meson scattering is normalized in such a way that

$$A(s,\mu^2,\mu^2) = \Delta^{\frac{1}{2}}(s,\mu^2,\mu^2)\,\sigma^{tot}(s,\mu^2,\mu^2)\,, \qquad (2.1)$$

where μ^2 is the meson mass squared, $\Delta(x,y,z) = x^2 + y^2 + z^2 - 2(xy + yz + zx)$, and σ^{tot} is the total meson-meson (μ-μ) cross section. The elastic μ-μ cross section σ^{el} enters in the input potential of the equation in the (on-shell) form

$$V(s_0,\mu^2,\mu^2) = \Delta^{\frac{1}{2}}(s_0,\mu^2,\mu^2)\sigma^{el}(s_0,\mu^2,\mu^2)\,. \qquad (2.2)$$

The $O(1,3)$ partial wave of A is defined as

$$A_\lambda(\tau_1,\tau_2) = \int_{4\mu^2}^{\infty} ds\; e^{-(\lambda+1)\theta(s,\tau_1,\tau_2)}\, A(s,\tau_1,\tau_2)\;; \qquad (2.3)$$

the inverse transform is

$$A(s,\tau_1,\tau_2) = \int_{c-i\infty}^{c+i\infty} \frac{d\lambda}{2\pi i}\, \frac{e^{+(\lambda+1)\theta(s,\tau_1,\tau_2)}}{2(-\tau_1)^{\frac{1}{2}}(-\tau_2)^{\frac{1}{2}}\sinh\theta(s,\tau_1,\tau_2)}\, A_\lambda(\tau_1,\tau_2)\,, \qquad (2.4)$$

where the contour is taken to the right of any singularity of A_λ in the λ plane. In terms of A_λ, the ABFST equation is

$$A_\lambda(\tau_1,\tau_2) = V_\lambda(\tau_1,\tau_2) + \frac{1}{16\pi^3(\lambda+1)}\int_{-\infty}^{0}\frac{d\tau'}{(\mu^2-\tau')^2} \times V_\lambda(\tau_1,\tau')\,A_\lambda(\tau',\tau_2)\,. \tag{2.5}$$

The essence of our method is to approximate

$$\frac{e^{-\theta(s,\tau_1,\tau_2)}}{(-\tau_1)^{\frac{1}{2}}(-\tau_2)^{\frac{1}{2}}} = \frac{2}{(s-\tau_1-\tau_2)+[(s-\tau_1-\tau_2)^2-4(-\tau_1)(-\tau_2)]^{\frac{1}{2}}} \tag{2.6}$$

by a factorizable expression[4]

$$\frac{\xi(s,\tau_1,\tau_2)}{(-\tau_1)^{\frac{1}{2}}(-\tau_2)^{\frac{1}{2}}} \equiv \frac{s}{(s-\tau_1)(s-\tau_2)}\,. \tag{2.7}$$

The function ξ is actually a lower bound to $e^{-\theta}$. Notice that

$$\frac{e^{-\theta(s,\tau_1,\tau_2)}}{(-\tau_1)^{\frac{1}{2}}(-\tau_2)^{\frac{1}{2}}} \to \frac{\xi(s,\tau_1,\tau_2)}{(-\tau_1)^{\frac{1}{2}}(-\tau_2)^{\frac{1}{2}}}\left[1+\frac{2(-\tau_1)(-\tau_2)}{s^2}\right] \tag{2.8}$$

when either τ_1 or τ_2, or both, approach zero. When τ_1 approaches (minus) infinity with τ_2 fixed, we have

$$\frac{e^{-\theta}}{(-\tau_1)^{\frac{1}{2}}(-\tau_2)^{\frac{1}{2}}} \to \frac{1}{(-\tau_1)}\,, \text{ whereas } \frac{\xi}{(-\tau_1)^{\frac{1}{2}}(-\tau_2)^{\frac{1}{2}}} \to \frac{1}{(-\tau_1)}\left(\frac{s}{s-\tau_2}\right).$$

The case is similar when τ_2 approaches (minus) infinity with τ_1 fixed. One hopes that, in any convergent integral involved in the calculation, the contributions from these "nonperipheral" regions do not matter very much. Notice also that ξ is a small quantity for all values of τ_1 and τ_2. For a given s, it has an absolute maximum

$$\xi(s,\tau_1,\tau_2)\Big|^{\text{abs.max.}}_{\tau_1=\tau_2=-s} = \frac{1}{4}\,, \tag{2.9}$$

whereas

$$e^{-\theta(s,\tau_1,\tau_2)}\Big|^{\text{max.}}_{\text{fixed }\tau_2,\,-\tau_1=s-\tau_2} = \frac{(s-\tau_2)^{\frac{1}{2}}-(s)^{\frac{1}{2}}}{(-\tau_2)^{\frac{1}{2}}} \le 1\,,$$

approaching the absolute maximum value of 1 for $-\tau_1 = -\tau_2 \gg s$.

With this approximation Eq. (2.5) is immediately soluble. Here we consider the solution for the kernel with a single (sharp) resonance. A kernel with many resonances will be discussed in subsection II.E. Thus we put for the (on-shell) potential

$$V(s_0,\mu^2,\mu^2) = \Delta^{\frac{1}{2}}(s_0,\mu^2,\mu^2)\pi m x\Gamma\,\sigma^{el}_{max}\delta(s_0-m^2) \equiv m^2R(0)\delta(s_0-m^2), \tag{2.10}$$

where m^2, x, and Γ are the squared mass, elasticity, and width of the μ-μ resonance. We shall assume $\mu^2 \ll m^2$. The solution to Eq. (2.5) is then

$$A_\lambda(\tau_1,\tau_2) = \frac{m^2R(0)\left[\dfrac{(-m^2\tau_1)^{\frac{1}{2}}(-m^2\tau_2)^{\frac{1}{2}}}{(m^2-\tau_1)(m^2-\tau_2)}\right]^{\lambda+1}}{1-\mathrm{Tr}K_\lambda}\,, \tag{2.11}$$

where

$$\mathrm{Tr}K_\lambda = \frac{m^2R(0)}{16\pi^3(\lambda+1)}\int_{-\infty}^{0}\frac{d\tau}{(\mu^2-\tau)^2}\left[\frac{-m^2\tau}{(m^2-\tau)^2}\right]^{\lambda+1}, \tag{2.12}$$

$$= \frac{R(0)}{16\pi^3}\,B(\lambda+2,\lambda+2)\,F\left(2\lambda+2,2\lambda+4,\,1-\frac{\mu^2}{m^2}\right), \tag{2.13}$$

$$= \frac{R(0)}{16\pi^3}\,\frac{B(\lambda,\lambda)}{2(2\lambda+1)}\,, \quad \text{for } \mu^2=0\,. \tag{2.14}$$

In Eq. (2.13) and Eq. (2.14), B is the Euler beta function and F is the hypergeometric function. The eigenvalue condition is given by the vanishing of the Fredholm determinant

$$D(\lambda) = 1 - \mathrm{Tr}K_\lambda = 0 . \tag{2.15}$$

A special property of this approximate solution is that, under the action of the original kernel, it "reproduces itself" for $-\tau_1$, $-\tau_2$, or both, small (in comparison with m^2). This can best be illustrated by going back to the s plane. From Eq. (2.4) and Eq. (2.11), we get for the leading behavior of the full amplitude

$$A(s,\tau_1,\tau_2) \underset{s\to\infty}{\sim} 16\pi^3 \beta_\alpha \left(\frac{m^2}{m^2-\tau_1}\right)^{\alpha+1} \left(\frac{m^2}{m^2-\tau_2}\right)^{\alpha+1} \left(\frac{s}{m^2}\right)^{\alpha} , \tag{2.16}$$

where α is the largest value of λ satisfying Eq. (2.15), and

$$\beta_\alpha = -\left[\frac{\partial}{\partial\lambda}\frac{16\pi^3}{R(0)}\mathrm{Tr}K_\lambda\right]^{-1}_{\lambda=\alpha} . \tag{2.17}$$

In the interest of simplicity and clarity, let us put $\mu^2 = 0$ for the moment; then the amplitude at the physical (and most peripheral) point is

$$A(s,0,0) \underset{s\to\infty}{\sim} 16\pi^3 \beta_\alpha \left(\frac{s}{m^2}\right)^{\alpha} . \tag{2.18}$$

On the other hand, in this asymptotic region of the s plane, the full amplitude, when written in the form

$$A(s,\tau_1,\tau_2) \underset{s\to\infty}{\sim} \phi_\alpha(\tau_1,\tau_2)s^\alpha , \tag{2.19}$$

satisfies an equation corresponding to Eq. (2.5)

$$[(-\tau_1)^{\frac{1}{2}}(-\tau_2)^{\frac{1}{2}}]^{\alpha+1}\,\phi_\alpha(\tau_1,\tau_2)$$

$$\sim \frac{1}{16\pi^3(\alpha+1)}\int ds_0 V(s_0,\tau_1,\tau') \int_{-\infty}^{0} \frac{d\tau'}{(\mu^2-\tau')^2} e^{-(\alpha+1)\theta(s_0,\tau_1,\tau')}$$

$$\times [(-\tau')^{\frac{1}{2}}(-\tau_2)^{\frac{1}{2}}]^{\alpha+1}\,\phi_\alpha(\tau',\tau_2) . \tag{2.20}$$

If we put Eq. (2.16) as a trial function into the right-hand side of Eq. (2.20) with the original kernel, the output physical amplitude is

$$A(s,0,0) \sim \lim_{\tau_1,\tau_2\to 0} \phi_\alpha(\tau_1,\tau_2)s^\alpha \tag{2.21}$$

$$\sim \frac{m^2R(0)}{16\pi^3(\alpha+1)} \int_{-\infty}^{0} \frac{d\tau'}{\tau'^2} \left(\frac{-\tau'}{m^2-\tau'}\right)^{\alpha+1} 16\pi^3 \beta_\alpha \left(\frac{m^2}{m^2-\tau'}\right)^{\alpha+1} \left(\frac{s}{m^2}\right)^{\alpha} \tag{2.22}$$

which is just Eq. (2.18) by virtue of Eq. (2.12) and Eq. (2.15). (Actually the condition $\tau_2 = 0$ is not necessary in this part of the argument; τ_2 can take any value.) The corresponding property can of course be demonstrated in the λ plane. It should be noted that some previously proposed approximate solutions[5-8] do not possess this property. Comparisons of the solution proposed here and other approximate solutions with the exact numerical solution will be given in subsection D.

C. THE NONFORWARD EQUATION AND ITS APPROXIMATE SOLUTION

Away from $t = 0$, the on-shell potential is given by

$$V(s_0,t) = \frac{1}{16\pi^2\Delta^{\frac{1}{2}}(s_0,\mu^2,\mu^2)}\int \frac{dt_1dt_2\theta\left(-\Delta(t,t_1,t_2) + \frac{4tt_1t_2}{s_0 - 4\mu^2}\right)}{\left[-\Delta(t,t_1,t_2) + \frac{4tt_1t_2}{s_0 - 4\mu^2}\right]^{\frac{1}{2}}} T^*(s_0,t_1)T(s_0,t_2), \tag{2.23}$$

where T is the complete elastic amplitude; $\text{Im } T(s,t) = A(s,t)$.

A single (sharp) resonance contributes a potential

$$V(s_0,t) = 2 \times \frac{16\pi s_0}{\Delta^{\frac{1}{2}}(s_0,\mu^2,\mu^2)}(2L + 1)P_L(z_s)\pi m\times\Gamma\delta(s_0 - m^2)$$

$$\equiv m^2R(t)\delta(s_0 - m^2) , \tag{2.24}$$

where

$$z_s = 1 + \frac{2s_0}{\Delta(s_0,\mu^2,\mu^2)}\, t$$

and L is the spin of the resonance.

The appropriate $O(1,2)$ partial-wave amplitude is

$$A_\ell(\tau_1,z_1,\tau_2,z_2;\, t) = \int_{4\mu^2}^{\infty} ds\, Q_\ell(\cosh\psi)\, A(\psi,\tau_1,z_1,\tau_2,z_2;\, t) , \tag{2.25}$$

and the inverse transform is

$$A(\psi,\tau_1,z_1,\tau_2,z_2;\, t) = \int_{c-i\infty}^{c+i\infty} \frac{d\ell}{2\pi i}\, \frac{(2\ell + 1)P_\ell(\cosh\psi)}{2[(-\tau_1)(1 - z_1^2)(-\tau_2)(1 - z_2^2)]^{\frac{1}{2}}} A_\ell(\tau_1,z_1,\tau_2,z_2;t), \tag{2.26}$$

where the contour is taken to the right of any singularity of A_ℓ in the ℓ plane.

In terms of A_ℓ, the nonforward ABFST equation is

$$A_\ell(\tau_1,z_1,\tau_2,z_2;\, t) = V_\ell(\tau_1,z_1,\tau_2,z_2;\, t) + \frac{1}{16\pi^4}\int_{-\infty}^{0} d\tau' \int_{-1}^{+1} \frac{dz'(1 - z'^2)^{-\frac{1}{2}}}{\left[(\mu^2 - \tau' - \frac{t}{4})^2 - \tau' t z'^2\right]} V_\ell(\tau_1,z_1,\tau',z';\, t)$$

$$\times A_\ell(\tau',z',\tau_2,z_2;\, t) . \tag{2.27}$$

In order to make an approximation similar to that discussed in subsection B, we note that the function $Q_\Delta(\cosh\psi)$ can be expanded as[9]

$$Q_\ell(\cosh\psi) = \sum_{n=0}^{\infty} \frac{\Gamma^2(\ell + 1)2^{2\ell+1}n!}{\Gamma(2\ell + 2 + n)} \left[(1 - z_1^2)^{\frac{\ell+1}{2}} C_n^{\ell+1}(z_1)\right] \times \left[(1 - z_2^2)^{\frac{\ell+1}{2}} C_n^{\ell+1}(z_2)\right] e^{-(\ell+1+n)\theta(s,\tau_1,\tau_2)} , \tag{2.28}$$

where $C_n^{\ell+1}$ is a Gegenbauer polynomial. Now, as before, we shall replace $e^{-\theta(s,\tau_1,\tau_2)}$ by $\xi(s,\tau_1,\tau_2)$ of Eq. (2.7). With the input potential Eq. (2.24), the kernel in Eq. (2.27) is then a sum of factorized terms. We shall discuss this case in subsection E. As a first approximation here, we take only the first term of the sum in

Eq. (2.28).[10] This is not unreasonable since, as we have realized above [Eq. (2.9)], $\xi(s,\tau_1,\tau_2)$ is a small quantity throughout the range of integration. Thus

$$\mathrm{Tr}K_\ell = \frac{m^2 R(t)\, B(\ell+1,\frac{1}{2})}{16\pi^4} \int_{-\infty}^{0} d\tau \int_{-1}^{+1} \frac{dz(1-z^2)^{\ell+\frac{1}{2}}}{[(\mu^2 - \tau - \frac{t}{4})^2 - \tau t z^2]}$$

$$\times \left[\frac{-m^2\tau}{(m^2-\tau)^2}\right]^{\ell+1}, \qquad (2.29)$$

$$= \frac{(m^2)^{\ell+2} R(t)}{16\pi^3(\ell+1)} \int_0^\infty du \frac{u^{\ell+1}}{(m^2+u)^{2\ell+2}} \frac{1}{(\mu^2+u+\zeta)^2}$$

$$\times F\left(1,\frac{1}{2},\ell+2,\frac{4u\zeta}{(\mu^2+u+\zeta)^2}\right), \qquad (2.30)$$

where we have used the notation $u = -\tau$ and $\zeta = -\frac{t}{4}$ for convenience. Now observe that, for a given $\zeta > 0$, the expression $(4u\zeta)/(\mu^2+u+\zeta)^2$ is always less than or equal to 1 throughout the range of integration

$$\left.\frac{4u\zeta}{(\mu^2+u+\zeta)^2}\right|_{u=\mu^2+\zeta}^{\text{max.}} = \frac{\zeta}{\mu^2+\zeta} < 1 \quad \text{for } \mu^2 \neq 0, \qquad = 1 \quad \text{for } \mu^2 = 0. \qquad (2.31)$$

Thus, the expansion of F as a hypergeometric series in powers of $(4u\zeta)/(\mu^2+u+\zeta)^2$ always stays within the radius of convergence of the series for $\mathrm{Re}\,\ell > -2$. After this expansion has been made, the series can be integrated term by term, each term being expressed as a hypergeometric function. Thus we get a series of hypergeometric functions with coefficients $(\zeta/m^2)^n$. The first two terms are as follows:

$$\mathrm{Tr}K_\ell = \frac{R(t)}{16\pi^3(\ell+1)} \left\{ B(\ell+2,\ell+2)\, F\left(2,\ell+2,2\ell+4,\ 1-\frac{\mu^2+\zeta}{m^2}\right) \right.$$

$$+ \frac{4}{2(\ell+2)}\left(\frac{\zeta}{m^2}\right) B(\ell+1,\ell+3)\, F\left(4,\ell+1,2\ell+4,1-\frac{\mu^2+\zeta}{m^2}\right)$$

$$\left. + O\left(\left(\frac{\zeta}{m^2}\right)^2 F\right)\right\} . \qquad (2.32)$$

The next step is to transform[11] $F(a,b,c,1-x)$ into $F(a',b',c',x)$ and then to express $F(a',b',c',x)$ as a hypergeometric series in powers of $x \equiv (\mu^2+\zeta)/(m^2)$ [since we shall be interested only in the small-t region where $(\mu^2+\zeta)/(m^2) \leq 1$]. After this manipulation, we obtain the eigenvalue condition

$$1 = \mathrm{Tr}K_\ell$$

$$= \frac{R(t)}{16\pi^3} \left\{ \frac{B(\ell,\ell)}{2(2\ell+1)} \left(1 + \frac{2(\ell+2)}{-\ell+1}\left(\frac{\mu^2+\zeta}{m^2}\right)\right.\right.$$

$$\left. + \frac{2(\ell+2)}{-\ell+1}\,\frac{3(\ell+3)}{-\ell+2}\,\frac{1}{2}\left(\frac{\mu^2+\zeta}{m^2}\right)^2 + \cdots\right)$$

$$\left. - \frac{\pi}{\sin\pi\ell}\left(\frac{\mu^2+\zeta}{m^2}\right)^\ell \right\}$$

$$\times \left(1 + \frac{(2\ell+2)(\ell+2)}{\ell+1}\left(\frac{\mu^2+\zeta}{m^2}\right) + \frac{(2\ell+2)(\ell+2)}{\ell+1}\,\frac{(2\ell+3)(\ell+3)}{\ell+2}\right.$$

$$\left. \times \frac{1}{2}\left(\frac{\mu^2+\zeta}{m^2}\right)^2 + \cdots\right)$$

Equation (2.33) Continued

Equation (2.33) Continued

$$+\frac{4}{2(\ell+2)}\left(\frac{\zeta}{m^2}\right)\left[-B(\ell,\ell)\,\frac{\ell}{-\ell+1}\left(\frac{1}{\ell+1}+\frac{4}{-\ell+2}\left(\frac{\mu^2+\zeta}{m^2}\right)+\cdots\right)\right.$$

$$+\frac{\ell(\ell+2)}{6}\,\frac{\pi}{\sin\pi\ell}\left(\frac{\mu^2+\zeta}{m^2}\right)^{\ell-1}\left(1+\frac{2\ell(\ell+3)}{\ell}\left(\frac{\mu^2+\zeta}{m^2}\right)+\cdots\right)\Bigg]$$

$$\left.+\,0\left(\left(\frac{\zeta}{m^2}\right)^2 F\right)\right\}\quad . \tag{2.33}$$

Notice that in Eq. (2.33), the radius of convergence of the series is controlled by m^2. Therefore, for $t \neq 0$, even if $\mu^2 \to 0$, the solution $\ell(t)$ of Eq. (2.33) remains finite. If, instead of the procedure following Eq. (2.30), a direct expansion of the nonforward propagator were made in the form

$$\frac{1}{[(\mu^2-\tau-\frac{t}{4})^2-\tau t z^2]}=\frac{1}{(\mu^2-\tau)^2}\left[1+\frac{t}{2}\,\frac{1}{(\mu^2-\tau)}-\frac{t\tau z^2}{(\mu^2-\tau)^2}+\cdots\right], \tag{2.34}$$

one would obtain a series representation of $\mathrm{Tr}K_\ell$ with a radius of convergence that is essentially controlled by μ^2. Thus such a procedure would suggest that $\mathrm{Tr}K_\ell \to \infty$ for $\mu^2 \to 0$ and $\ell < 1$, even though the corresponding integral representation of $\mathrm{Tr}K_\ell$ is actually finite in this limit.[6,8]

The slopes of the trajectories can easily be computed from Eq. (2.33) by the formula

$$\frac{d\ell}{dt}=-\frac{\partial \mathrm{Tr}K_\ell}{\partial t}\Big/\frac{\partial \mathrm{Tr}K_\ell}{\partial \ell}\ .$$

Thus

$$\left.\frac{d\alpha}{dt}\right|_{t=0}=\frac{1}{Y(0)}\left[\frac{1}{4m^2}X(0)-\frac{16\pi^3}{R(0)}\cdot\left(\frac{2m^2}{\Delta(m^2,\mu^2,\mu^2)}\right)P_L'(1)\right] \tag{2.35}$$

in which α satisfies Eq. (2.33) and

$$X(0)=\left[\frac{\partial}{\partial\zeta}\,\frac{16\pi^3}{R(t)}\,\mathrm{Tr}K_\ell\right]_{\ell=\alpha(0),\,\zeta=0} \tag{2.36}$$

$$=\frac{B(\alpha,\alpha)(\alpha+2)}{(-\alpha+1)(2\alpha+1)}\left[1+\frac{3(\alpha+3)}{(-\alpha+2)}\left(\frac{\mu^2}{m^2}\right)+\cdots\right]$$

$$-\frac{\pi}{\sin\pi\alpha}\left(\frac{\mu^2}{m^2}\right)^{\alpha-1}\left[\alpha+2(\alpha+1)(\alpha+2)\left(\frac{\mu^2}{m^2}\right)+\cdots\right]$$

$$-\frac{2\alpha\,B(\alpha,\alpha)}{(-\alpha+1)(\alpha+1)(\alpha+2)}\left[1+\frac{4(\alpha+1)}{(-\alpha+2)}\left(\frac{\mu^2}{m^2}\right)+\cdots\right]$$

$$+\frac{\pi}{\sin\pi\alpha}\,\frac{\alpha}{3}\left(\frac{\mu^2}{m^2}\right)^{\alpha-1}\left[1+2(\alpha+3)\left(\frac{\mu^2}{m^2}\right)+\cdots\right], \tag{2.37}$$

$$\overline{\overline{\alpha=1}}\quad\left(\frac{43}{18}+\frac{2}{3}\log\left(\frac{\mu^2}{m^2}\right)\right)+\left(\frac{169}{9}+\frac{28}{3}\log\left(\frac{\mu^2}{m^2}\right)\right)\left(\frac{\mu^2}{m^2}\right)+\cdots\ , \tag{2.38}$$

$$Y(0) = \left[\frac{\partial}{\partial \ell}\frac{16\pi^3}{R(t)}\,\mathrm{Tr}K_\ell\right]_{\ell=\alpha(0),\zeta=0} \tag{2.39}$$

$$= \left(\frac{\dot{B}(\alpha,\alpha)}{2(2\alpha+1)} - \frac{B(\alpha,\alpha)}{(2\alpha+1)^2}\right)$$

$$+ \left(\frac{\dot{B}(\alpha,\alpha)(\alpha+2)}{(-\alpha+1)(2\alpha+1)} - \frac{3B(\alpha,\alpha)}{(-\alpha+1)(2\alpha+1)^2}\right.$$

$$\left. + \frac{B(\alpha,\alpha)(\alpha+2)}{(-\alpha+1)^2(2\alpha+1)}\right)\left(\frac{\mu^2}{m^2}\right) + \cdots$$

$$+ \left[\frac{-\pi}{\sin\pi\alpha}\left(\frac{\mu^2}{m^2}\right)^\alpha \log\left(\frac{\mu^2}{m^2}\right) + \left(\frac{\pi}{\sin\pi\alpha}\right)^2(\cos\pi\alpha)\left(\frac{\mu^2}{m^2}\right)^\alpha\right]$$

$$\times\left(1 + 2(\alpha+2)\left(\frac{\mu^2}{m^2}\right) + \cdots\right) - 2\frac{\pi}{\sin\pi\alpha}\left(\frac{\mu^2}{m^2}\right)^{\alpha+1} + \cdots, \tag{2.40}$$

$$\overline{\alpha=1} \quad -\frac{4}{9} - \frac{1}{2}\left(\frac{67}{9} - \frac{\pi^2}{3} - \log^2\left(\frac{\mu^2}{m^2}\right)\right)\left(\frac{\mu^2}{m^2}\right) - \cdots . \tag{2.41}$$

In Eq. (2.40), $\dot{B}(\alpha,\alpha) = 2B(\alpha,\alpha)[\Psi(\alpha) - \Psi(2\alpha)]$. From these relations one sees immediately that owing to the presence of the factor $[(\mu^2)/(m^2)]^{\alpha-1}$ in $X(0)$, $(d\alpha)/(dt)|_{t=0} \to \infty$ when $\mu^2 \to 0$ and $\alpha \leq 1$. Alternatively one can see this from the derivative of the integral representation of $\mathrm{Tr}K_\ell$ in Eq. (2.30): The integral $[\partial/(\partial\zeta)]\mathrm{Tr}K_\ell$ diverges at the lower end of integration when $\mu^2 = 0$ and $\zeta = 0$. By taking $\mu^2 \to 0$ we have moved the threshold from $t = 4\mu^2 > 0$ to $t = 0$.

We also have

$$A_\ell(\tau_1,z_1,\tau_2,z_2;\,t) = \frac{B(\ell+1,\frac{1}{2})[(1-z_1^2)(1-z_2^2)]^{\frac{\ell+1}{2}}R(t)}{1-\mathrm{Tr}K_\ell}\left[\frac{(-m^2\tau_1)^{\frac{1}{2}}(-m^2\tau_2)^{\frac{1}{2}}}{(m^2-\tau_1)(m^2-\tau_2)}\right]^{\ell+1}, \tag{2.42}$$

$$A(s,\tau_1,\tau_2;\,t) \underset{s\to\infty}{\sim} 16\pi^3\,\beta_{\alpha(t)}(t) \times\left(\frac{m^2}{m^2-\tau_1}\right)^{\alpha(t)+1}\left(\frac{m^2}{m^2-\tau_2}\right)^{\alpha(t)+1}\left(\frac{s}{m^2}\right)^{\alpha(t)}, \tag{2.43}$$

where, as before, $\beta_{\alpha(t)}(t) = -[Y(t)]^{-1}$.

Notice that when t (i.e., ζ) goes to zero, Eq. (2.43) coincides with Eq. (2.16). That is, in the forward limit, the leading member of the family of Regge poles ($\ell = \alpha - n$, $n = 0,1,2,\cdots$) and the corresponding Toller pole ($\lambda = \alpha$) are the same, as far as the high-energy behavior of the full amplitude is concerned. This result is true in general and does not depend on the approximation we have made. On the other hand, from Eq. (2.42) and Eq. (2.11) we see that $A_\ell \xrightarrow[t\to 0]{} A_\lambda$ apart from the function $B(\ell+1,\frac{1}{2})$ and a factor with dependence on z_1 and z_2; however, this result follows only from the fact that we have discarded all the daughters ($\ell = \alpha - 1, \alpha - 2, \cdots$) in A_ℓ,[9] owing to the approximation made after Eq. (2.28).

D. EXACT NUMERICAL SOLUTION AND COMPARISON WITH APPROXIMATE SOLUTIONS

We have also solved Eq. (2.5) and Eq. (2.27) numerically, using the method described by Wyld[12] to find the leading pole and its residue. We have considered the two cases $\mu^2 = 0$ and $\mu^2 = m_\pi^2$ (i.e., $\mu^2/m^2 = 1/30$) for a kernel consisting of a sharp resonance of mass squared $m^2 = m_\rho^2 = 0.585$ GeV^2. The quantity R is treated as a variable parameter.

In Fig. 3 we show the numerical solution for the intercept of the leading pole when $\mu^2 = 0$. It should be noted that the method of numerical solution is not precise in this zero μ limit: the error in α might be as high as ± 0.1. The value of $\alpha(0)$ calculated from Eq. (2.33) with $\mu^2 = 0$ and $\zeta = 0$ is also plotted; it differs from the numerical solution by about 6% when $\alpha = 1$. For the sake of comparison we have also plotted the values of $\alpha(0)$ calculated in the trace approximation[2]

$$1 = \frac{R(0)}{16\pi^3} \frac{2}{\alpha(\alpha+1)(\alpha+2)} \tag{2.44}$$

(dashed line), and the approximate solution of Ref. 5

$$1 = \frac{R(0)}{16\pi^3} \frac{1}{\alpha(\alpha+1)} \tag{2.45}$$

(dotted line), which is also the expression obtained in Ref. 6.

Figure 4 shows the numerical solution for $\alpha(0)$ when $(\mu^2)/(m^2) = 1/30$, together with the value of $\alpha(0)$ calculated from Eq. (2.33) to first order in $(\mu^2)/(m^2)$.

Figure 5 shows the numerical solution for the residue of the leading pole defined in Eq. (2.19) when $\mu^2 = 0$. In this figure we have also plotted our approximate solution from Eq. (2.18)

$$\phi_\alpha(0,0) \sim 16\pi^3 \beta_\alpha \frac{1}{(m^2)^\alpha} , \tag{2.46}$$

where $\beta_\alpha(0) = -[Y(0)]^{-1}$ with $\mu^2 = 0$ in Eq. (2.39). Again we also show the value of $\phi_\alpha(0,0)$ calculated from Ref. 7 (dashed line) and from the eigenvalue condition [our Eq. (2.45)] of Refs. 5 and 6 (in dotted line). For $[R(0)]/(16\pi^3) = 4$, say, Eq. (2.46) misses the exact solution by about 10%, whereas the other approximate solutions miss by more than 100%.

In Fig. 6 we show the numerical solution for $\phi_\alpha(0,0)$ when $(\mu^2)/(m^2) = 1/30$. The approximate solution given by Eq. (2.46) with $\beta_\alpha = -[Y(0)]^{-1}$ is also shown to first order in $(\mu^2)/(m^2)$.

Figure 7 shows the off-shell dependence of the residue of the leading pole when $\mu^2 = 0$. From Eq. (2.16), we have

$$\phi_\alpha(\tau_1,0) = \phi_\alpha(0,0)\left(\frac{m^2}{m^2 - \tau_1}\right)^{\alpha+1} . \tag{2.47}$$

It is seen that the approximate solutions are "more peripheral" than the exact ones. This is not surprising since we have replaced the original kernel by the one which is more peripheral [c.f., Eq. (2.6) and Eq. (2.7)].

Finally, in Fig. 8 we show the slope of the leading pole at $t = 0$, when the μ-μ resonance is (i) a scalar and (ii) a vector. The numerical solution for $t = 0$ lies somewhere within the shaded area. We have also computed the values of the slope at $t = 0$

according to Eq. (2.35) up to order $[(\mu^2)/(m^2)]^2$ at three different values of $R(0)$ corresponding to $\alpha(0) = 0.5$, 0.8, and 1.0.[13] They are shown as X's in the figure.

E. GENERALIZATIONS

Let us consider briefly the case of a kernel consisting of a finite sum of factorized (and symmetric) terms. The sum may arise either from the input of many resonances in Eq. (2.10) or from taking more terms in the series of Eq. (2.28). For example, if we put $V(s,\mu^2,\mu^2) = \sum_{i=1}^{n} m_i^2 R_i \delta(s - m_i^2)$, then we have

$$V_\lambda(\tau_1,\tau_2) = \sum_i \left[m_i R_i^{\frac{1}{2}} \left(\frac{m_i(-\tau_1)^{\frac{1}{2}}}{m_i^2 - \tau_1} \right)^{\lambda+1} \right] \left[m_i R_i^{\frac{1}{2}} \left(\frac{m_i(-\tau_2)^{\frac{1}{2}}}{m_i^2 - \tau_2} \right)^{\lambda+1} \right], \tag{2.48}$$

which is no longer factorizable in τ_1 and τ_2. The resulting equation can be solved by an algebraic method. That is, for an integral equation of the type

$$f(\tau_1,\tau_2) = V(\tau_1,\tau_2) + \int V(\tau_1,\tau') S(\tau') f(\tau',\tau_2) d\tau' \tag{2.49}$$

with $V(\tau_1,\tau_2) = \sum_{i=1}^{n} v_i(\tau_1) v_i(\tau_2)$, the solution is just

$$f(\tau_1,\tau_2) = \sum_{i=1}^{n} v_i(\tau_1) v_i(\tau_2) + \sum_{i,j,k=1}^{n} v_i(\tau_1) (1 - T)^{-1}_{ij} T_{jk} v_k(\tau_2), \tag{2.50}$$

where

$$T_{ij} = T_{ji} = \int v_i(\tau) S(\tau) v_j(\tau) d\tau . \tag{2.51}$$

For the case $n = 2$, for example, the solution is

$$f(\tau_1,\tau_2)$$

$$= [(1 - T_{22})v_1(\tau_1)v_1(\tau_2) + (1 - T_{11})v_2(\tau_1)v_2(\tau_2) + T_{12}v_1(\tau_1)v_2(\tau_2)$$

$$+ T_{21}v_2(\tau_1)v_1(\tau_2)][(1 - T_{11})(1 - T_{22}) - T_{12}T_{21}]^{-1}, \quad (2.52)$$

which is similar to the solution to a coupled-channel problem.

F. DISCUSSION

From the explicit approximate solution, Eq.(2.16), Eq. (2.33), and Eqs. (2.35-43), we see the following characteristics:

(1) The leading behaviors of the trajectory and residue do not depend on the external mass μ^2; in fact, the full expressions for them remain finite in the limit $\mu^2 \to 0$ (but not for the slope at $t = 0$ for $\alpha \leq 1$).

(2) The mass m^2 plays the role of the "scale parameter" in the factor $[(s)/(m^2)]^\alpha$ as well as in the slope formula Eq. (2.35); this scale parameter is usually asserted to be about 1 GeV^2 in Regge phenomenology. And, apart from the masses μ^2 and m^2, the residue is completely determined by the location of the pole $\alpha(t)$. [In the Veneziano model, the situation is similar to that mentioned in (2) above, in that it is the reciprocal of the slope of the trajectories which serves as the scale parameter. But in that model there is an overall factor in the residues (the constant usually denoted by β) which is not determined by the theory itself.] Most important of all, the absolute magnitude of high energy total cross section so determined turns out to be a resonable value when an appropriate symmetry scheme is incorporated into the model. We shall illustrate this point in Sec. III below.

(3) The high energy off-shell "form factor" given by Eq. (2.16) or Eq. (2.43) is an interesting output from this model. Its theoretical and phenomenological implications will be discussed in Sec. IV.

From the numerical solution (as well as from the approximate solution), we see that the leading pole position $\alpha(0)$ and the residue ϕ_α display monotonic behavior as a function of the kernel strength, which is characterized by $R(0)/16\pi^3$. As we have mentioned

in subsection B, the factorizable expression (2.7) we used is actually a lower bound to the original kernel (2.6), whereas the approximate solutions obtained by various authors[5-8] are based on some upper bound factorizable expressions. It can be shown[14] that, for $\alpha(0)$, the approximate value obtained here is a lower bound to the exact one, while other approximate values[5-8] are its upper bounds.[15]

Let us now turn to the question of the uniqueness of our approximation scheme. As we have understood, there exist a lot of factorizable forms similar to the particular one given in Eq. (2.29). Even the conditions that we imposed in Eq. (2.8) and Eq. (2.22) do not seem to determine $\xi(s,\tau_1,\tau_2)$ uniquely. However, if we multiply Eq. (2.7) by a factor $\gamma(s,\tau_1)\gamma(s,\tau_2)$ in which we require $\gamma(m^2,\tau_1)\gamma(m^2,\tau_2) = 1$ when either τ_1 or τ_2 goes to zero, [i.e., that $\xi(m^2,\tau_1,\tau_2)\gamma(m^2,\tau_1)\gamma(m^2,\tau_2)$ matches $e^{-\theta(s,\tau_1,\tau_2)}$ along the line $\tau_1 = 0$ ($\tau_2 = 0$) for all values of τ_2 (τ_1) in the τ_1 - τ_2 plane], then it must be true that $\gamma(m^2,\tau) \equiv 1$ (apart from a sign). On the other hand, if we only require $\gamma(m^2,0) = 1$, then the condition in Eq. (2.22) imposes

$$\int_{-\infty}^{0} \frac{d\tau}{\tau^2}\left[\frac{-m^2\tau}{(m^2-\tau)^2}\right]^{\lambda+1}[\gamma^2(m^2,\tau) - \gamma(m^2,\tau)] = 0 . \qquad (2.53)$$

Of course $\gamma(m^2,\tau) \equiv 1$ (the original proposal) fulfills this requirement. There do exist, however, non-null functions which are orthogonal to $1/\tau^2[(-m^2\tau)/(m^2-\tau)^2]^{\lambda+1}$; and thus one may be able to choose a suitable $\gamma(m^2,\tau)$ to match the high τ behavior of $e^{-\theta(s,\tau_1,\tau_2)}$. We shall not investigate this possibility further here. It suffices to say that Eq. (2.7) seems to be the simplest choice and produces a

solution with reasonable analytic properties and in fairly good numerical agreement with the exact solution. We believe that such a solution will be useful in the semi-quantitative study of the general physical output of the multiperipheral model.[16]

III. AN APPLICATION: CALCULATION OF THE MAGNITUDE OF HIGH ENERGY MESON-BARYON TOTAL CROSS SECTION

In this section,[17] we shall incorporate internal symmetry into the scheme. And we shall study, in a somewhat crude way, the forward scattering between a pseudoscalar meson (μ) and a baryon (B) at very high energy on the basis of the approximate solution obtained in Sec. II. This study is inspired by Ref. 7 in which an order-of-magnitude calculation of μ-μ total cross section from a multiperipheral model is done using the trace approximation solution. The purpose of the present work is to extend the calculation to a "physical" process, using a more accurate solution and handling (at least formally) the spin complication. We shall be able to see how far our output differs from the observed values at the presently highest available energy. The physical significance of these semiquantitative calculations will be discussed at the end of this section.

Since here we are not interested in the precise numerical value of the output from the model, we shall make the following simplifications. We believe that we do not lose the essence of the physics in doing these:

(1) We assume an exact SU(n) internal symmetry in the dynamics. The equation is then diagonalized in the t-channel quantum numbers. And the Pomeranchuk pole is assumed to belong to a singlet representation in the t-channel. In practice, it turns out that the symmetry should be SU(3), in order to get the output magnitude of σ^{tot} to be a reasonable value in comparison with experiments or expectations. This corresponds to the maximal generalization of the original pion-exchange model without possibly altering the form of the equation by including,

e.g., vector meson exchange. An SU(2)-symmetric model, ignoring the existence of strange mesons and baryons, not only suffers from the difficulty that the π-π kernel is too weak to produce[2,18] $\alpha(0) \approx 1$ for the leading vacuum pole, but also gives a result for σ^{tot} almost an order of magnitude too great.

(2) From Eq. (2.2), the (on-shell) input μ-μ kernel is

$$V^{I_t}(s_0,\mu^2,\mu^2) = \sum_{I_s} X^{I_t,I_s} \Delta^{\frac{1}{2}}(s_0,\mu^2,\mu^2)\, \sigma^{el,I_s}(s_0,\mu^2,\mu^2) \ , \quad (3.1)$$

where I_t, I_s are the quantum number index in t,s channels respectively, and X^{I_t,I_s} is the crossing matrix element. Accurate numerical study,[19] inputting all the observed μ-μ resonances together with some off-shell corrections to that, shows the eigenvalue $\alpha(0)$ to be about 0.7. It is conceivable that various other delicate corrections, if taken into account, might even push this value higher. But here we simply put (for $I_t = 1$),

$$V^1(s_0,\mu^2,\mu^2) = m_0^2 R^1 \delta(s_0 - m_0^2) \ , \quad (3.2)$$

and assume the value of R^1 gives $\alpha(0) = 1$. This rough approximation amounts to, essentially, replacing the detail spectrum of the low energy μ-μ resonances which have squared masses around 1 GeV^2, with a single resonance located at $s_0 = m_0^2$ and with all the "weights" attached to it. (Recall that m_0^2 will also serve as the scale factor in the output high energy amplitude.) Correspondingly we replace the sum in V_λ of Eq. (2.48), in which each term has the same functional behavior, by a single representing term.

(3) We neglect μ^2 in comparison with all other masses in question. As we have seen in Sec. II, this is a good approximation as long as $\alpha(0) \gtrsim \frac{1}{2}$.

(4) Assuming the production amplitudes of μB scattering to be given by Fig. 9a for even numbers of final μ's, and by Fig. 9b for odd numbers of final μ's, we approximate the low energy μB kernel by a B pole plus the first prominent μB resonance pole. This approach is motivated by known facts about $\sigma_{\mu B}^{el}$, like the curves shown in Fig. 10. Thus we have[20]

$$V_{\mu B}{}^{1}(s_B,\tau') = \sum_{I_s} X^{1,I_s} z_{I_s} \pi(-\tau') g^2\left(\frac{r^{-2}}{r^{-2}-\tau'}\right) \delta(s_B - M^2)$$

$$+ X^{1,R} \Delta^{\frac{1}{2}} \pi m_R x_R \Gamma_R \sigma_{\mu B}^{el,R}(\max) \delta(s_B - m_R^2) , \qquad (3.3)$$

where both sides refer to spin-averaged quantities. The factor z_{I_s} comes from the projection of the symmetry factor, e.g., $(\tau_f\tau_i)_{f=i}$ onto the subspace with quantum number I_s in the s-channel. The factor $\left(r^{-2}/(r^{-2}-\tau')\right)$ is the Dürr-Pilkuhn form factor[21] for the μ-B-B vertex, and r is the "radius" parameter of the vertex. We cannot keep this vertex on-shell because that will make it negative. The prescription of vertices in Eq. (3.3) gives a satisfactory description of experimental differential cross sections in singly peripheral reactions at low energy. For example, the reactions $\pi N \to \rho N$ and $\pi N \to \rho\Delta$ at $p_{lab}^{\pi} = 4$ GeV/c [for which we use OPE models with ρ vertices on-shell, in addition to the prescription Eq. (3.3) for the N and Δ vertices]. This problem has been

discussed in Ref. 17. The reader is referred to that reference for detail.

After this long preparation, we are now ready to calculated the high energy forward elastic μB amplitude. From Eq. (2.20) and Eq. (2.22), we have

$$A_{\mu B}{}^{1}(s,M^2,0)$$

$$\sim \frac{1}{16\pi^3(\alpha+1)} \int ds_B \, V_{\mu B}{}^{1}(s_B,\tau') \int_{-\infty}^{0} \frac{d\tau'}{\tau'^2} e^{-(\alpha+1)\theta(s_B,M^2,\tau')}$$

$$\times \left(\frac{-\tau'}{-M^2}\right)^{\frac{\alpha+1}{2}} A^{1}(s,\tau',0) \qquad (3.4)$$

where $A^1(s,\tau',0)$ is given by Eq. (2.16). Next, recall that, as far as internal symmetry $SU(n)$ is concerned, any elastic amplitude in the direct at high energy at or near the forward direction is related to the crossed-channel amplitude which corresponds to the identity representation by[22]

$$T_{\mu B} \sim \frac{1}{N_\mu^{\frac{1}{2}} N_B^{\frac{1}{2}}} T_{\mu B}{}^{1} \qquad (3.5)$$

when $T_{\mu B}{}^{1}$ dominates other amplitudes in the crossed channel. The factor $N_\mu^{-\frac{1}{2}} N_B^{-\frac{1}{2}}$ comes from the s-t crossing matrix and N_μ (N_B) is the dimension of the subspace to which μ(B) belongs. Combining Eq. (3.3), Eq. (3.4), and Eq. (3.5), we have

$$\sigma_{\mu B}^{tot} \underset{s\to\infty}{\sim} \frac{1}{s} \frac{1}{N_\mu^{\frac{1}{2}} N_B^{\frac{1}{2}}} A_{\mu B}^{1}$$

$$\underset{s\to\infty}{\sim} \frac{1}{N_\mu^{\frac{1}{2}} N_B^{\frac{1}{2}}} \sum_{I_s} X^{1,I_s} z_{I_s} \pi g^2 \vartheta_{1B}/m_0^2$$

$$+ \frac{1}{N_\mu^{\frac{1}{2}} N_B^{\frac{1}{2}}} X^{1,R} x_R \pi m_R \Gamma_R \sigma_{\mu B}^{el,R}(max) \vartheta_{1R}/m_0^2 , \qquad (3.6)$$

where the dimensionless quantities

$$\vartheta_{1B} = \frac{\beta_1 m_0^4}{(2M^2)^2} \int_{-\infty}^{0} d\tau' \frac{1}{\tau'^2(m_0^2 - \tau')^2} \frac{(-\tau')r^{-2}}{(r^{-2} - \tau')}$$

$$\times [(\tau'^2 - \tilde{b}\tau') + \tau'(\tau'^2 - 2\tilde{b}\tau')^{\frac{1}{2}}] , \qquad (3.7)$$

$$= \frac{\beta_1}{b^2}\left(\frac{r^2}{(r^2-1)^2}\left\{(b - r^2)\ell n \frac{b}{2r^2} + \frac{2br^2 - r^4}{(2br^2 - r^4)^{\frac{1}{2}}}\right.\right.$$

$$\left.\times \left[\sin^{-1}\left(1 - \frac{r^2}{b}\right) + \sin^{-1}(1)\right]\right\}$$

$$- \frac{r^2}{(r^2-1)^2}\left\{(b-1)\ell n \frac{b}{2} + \frac{2b-1}{(2b-1)^{\frac{1}{2}}}\left[\sin^{-1}\left(1 - \frac{1}{b}\right) + \sin^{-1}(1)\right]\right\}$$

$$\left.+ \frac{r^2}{(r^2-1)}\left\{b + \ell n \frac{b}{2} - \frac{b-1}{(2b-1)^{\frac{1}{2}}}\left[\sin^{-1}\left(1 - \frac{1}{b}\right) + \sin^{-1}(1)\right]\right\}\right) , \qquad (3.8)$$

$$\vartheta_{1B} = \frac{\beta_1}{b^2}\left\{\frac{b^2}{2b-1} - \frac{b^2}{2(2b-1)^{3/2}}\left[\sin^{-1}\left(1 - \frac{1}{b}\right) + \sin^{-1}(1)\right]\right\}$$

$$\text{for } r^{-2} = m_0^2 , \qquad (3.9)$$

with

$$b = \frac{\tilde{b}}{m_0^2} = \frac{2M^2}{m_0^2} , \qquad r = \frac{r^{-2}}{m_0^2} ,$$

and

$$\vartheta_{IR} = \frac{\beta_1 m_0^4}{(2M^2)^2} \int_{-\infty}^{0} d\tau' \frac{\tilde{a}}{\tau'^2(m_0^2 - \tau')^2}$$

$$\times \{[\tau'^2 - (\tilde{a} + \tilde{b})\tau' + \tilde{a}^2] - (\tilde{a} - \tau')(\tau'^2 - 2\tilde{b}\tau' + \tilde{a}^2)^{\frac{1}{2}}\} \qquad (3.10)$$

$$= \frac{\beta_1 a}{b^2}\left\{2(a-b) + (a + b - 2a^2)\ell n \frac{a+b}{2a^2}\right\}$$

$$\left.+ \frac{-a - b + 3ba + a^2 - 2a^3}{(2b - 1 - a^2)^{\frac{1}{2}}}\left[\sin^{-1}\frac{b - a^2}{(b^2 - a^2)^{\frac{1}{2}}} + \sin^{-1}\frac{b-1}{(b^2-a^2)^{\frac{1}{2}}}\right]\right\} \qquad (3.11)$$

with

$$a = \frac{\tilde{a}}{m_0^2} = \frac{m_R^2}{m_0^2} - \frac{M^2}{m_0^2} , \qquad b = \frac{\tilde{b}}{m_0^2} = \frac{m_R^2}{m_0^2} + \frac{M^2}{m_0^2} .$$

It is noteworthy that the behavior of the integrands in Eq. (3.7) and Eq. (3.10) are similar. In the two limits of integration,

integrand of Eq. (3.7) $\xrightarrow[\tau'\to 0]{} \frac{\tilde{b}}{m_0^4}$, $\underset{\tau'\to -\infty}{\sim} \frac{\frac{1}{2} r^{-2} \tilde{b}^2}{\tau'^4}$; $\tilde{b} = 2M^2$,

(3.12)

integrand of Eq. (3.10) $\xrightarrow[\tau'\to 0]{} \frac{\frac{1}{2} \tilde{a}[(\tilde{b} - \tilde{a})/\tilde{a}]^2}{m_0^4}$,

$$\underset{\tau'\to -\infty}{\sim} \frac{\frac{1}{2} \tilde{a}(\tilde{b}^2 + \tilde{a}^2)}{\tau'^4} ; \qquad \begin{aligned} \tilde{a} &= m_R^2 - M^2 , \\ \tilde{b} &= m_R^2 + M^2 . \end{aligned} \tag{3.13}$$

They both decrease monotonically from a finite value to zero and fall off asymptotically $\propto \tau'^{-4}$. Thus B and R contribute to the right-most (Fig. 9a and 9b) links with the same degree of "peripherality." Without the help of the Dürr-Pilkuhn form factor for the B-pole vertex, the integrand of Eq. (3.7) would fall off like τ'^{-3} and thus make the B contribution much less peripheral than the R contribution.

Numerical Value of the Asymptotic $\sigma^{tot}_{\mu B}$ in an SU(3)-symmetric Model:

We adopt the following as our "best input" for the hypothetical exact-SU(3)-symmetry limit. Consider μ, M, and m_R to be the $0^-\underset{\sim}{8}(K, \pi, \eta, \bar{K})$, $\frac{1}{2}^+\underset{\sim}{8}(N, \Sigma, \Lambda, \Xi)$, and $\frac{3}{2}^+\underset{\sim\sim}{10}(\Delta, \Sigma, \Xi, \Omega)$ respectively, and take, for definiteness, m_0 to be m_V $1^-\underset{\sim}{8}(K^*, \rho, \phi, \bar{K}^*)$. The mixing of $\underset{\sim}{1}$ and $\underset{\sim}{8}$ is ignored. We continue to set the mass of μ equal to zero. But for other mass, we use the first term in the corresponding Gell-Mann-Okubo mass formula.[23] Thus M = 1.15 GeV, m_R = 1.385 GeV, and $m_0 = m_V$ = 0.852 GeV.

For the B vertex, we now have

$$z_{I_s} = \{4[\alpha^2 D_f D_i + (1 - \alpha)^2 F_f F_i + \alpha(1 - \alpha)(D_f F_i + F_f D_i)]_{f=i}\}_{I_s} , \tag{3.14}$$

where $I_s = 8_{ss}$, 8_{aa}, 8_{sa}, and 8_{as}, and $D_f D_i = \frac{5}{3}(\mathcal{P}_{8_{ss}})_{fi}$, $F_f F_i = 3(\mathcal{P}_{8_{aa}})_{fi}$, etc. (the $\mathcal{P}$'s are projection operators for the corresponding subspaces). We use the D/F ratio $\alpha = \frac{2}{3}$ and $g^2 = 14.4 \times 4\pi$. We furthermore choose[24] $r^{-2} = \frac{1}{2} m_0^2$.

For the R vertex, we use the calculated value of the width Γ_R from the SU(3) Chew-Low static model,[25,26]

$$\Gamma_R = 2 \times \frac{2}{3} \times \frac{8}{3} \alpha(3 - 2\alpha) \frac{g^2}{4\pi} \frac{1}{4M^2} p^3_{c.m.} \approx 0.107 \text{ GeV}, \tag{3.15}$$

and we put $x_R = 1$.

Recall finally that $N_\mu = 8$, $N_B = 8$, $X^{1,8_{ss}} = X^{1,8_{aa}} = 1$, $X^{1,8_{sa}} = X^{1,8_{as}} = 0$ $\left(\text{thus } \sum_{I_s} z_{I_s} = \frac{116}{27}\right)$, $X^{1,10} = \frac{5}{4}$. And from Eq. (2.17), we get $\beta_1 = \frac{9}{4}$.

Feeding all these ingredients into the right-hand side of Eq. (3.6), we obtain

$$\sigma^{tot}_{\mu B} \underset{s\to\infty}{\sim} 30.9 \text{ mb}. \tag{3.16}$$

This value is comparable to the Serpukhov data[27] $\sigma^{tot}_{\pi^- p} \underset{65 \text{ GeV/c}}{\sim} 24.69$ mb, $\sigma^{tot}_{K^- p} \underset{55 \text{ GeV/c}}{\sim} 21.5$ mb, or to the projected values[28] $\sigma^{tot}_{\pi N} \sim 21$ mb, and $\sigma^{tot}_{KN} \sim 17.2$ mb.

We conclude this section with these remarks:

(1) With multiperipheral dynamics, the absolute magnitudes of high energy scattering cross sections are calculable. And these magnitudes are determined decisively by the properties of a few low-lying states.

(2) To get these magnitudes about right, it is important to count properly the symmetry-multiplet structure of the reacting hadrons.

(3) If we input more μB resonances in Eq. (3.3), we shall probably make the output in Eq. (3.16) even larger. On the other hand, if we use Eq. (2.18) and calculate $\sigma_{\mu\mu}^{tot}$ in this oversimplified way, we get a value a couple times larger than the value expected from factorization. The main deficiency of the scheme we developed so far is, we believe, that we have not included the high energy scattering part in the input in V. This question will be addressed in Sec. V.

IV. HIGH ENERGY OFF-SHELL BEHAVIOR

Referring back to Fig. 2 and Table 1, we see that the masses of the four legs of amplitude A are related to other variables by

$$\mu_{1+}^2 = \left(\frac{q}{2} + p_1\right)^2 = \tau_1 + \frac{t}{4} + (-\tau_1)^{\frac{1}{2}}(-t)^{\frac{1}{2}} z_1 , \qquad (4.1)$$

$$\mu_{1-}^2 = \left(\frac{q}{2} - p_1\right)^2 = \tau_1 + \frac{t}{4} - (-\tau_1)^{\frac{1}{2}}(-t)^{\frac{1}{2}} z_1 \qquad (4.2)$$

for the left legs, and similar relations for the right legs. So we may express the variables τ_1, z_1 etc. in terms of the masses, e.g.

$$\tau_1 = \frac{1}{2}\left[\left(\mu_{1+}^2 - \frac{t}{4}\right) + \left(\mu_{1-}^2 - \frac{t}{4}\right)\right] , \qquad (4.3)$$

$$z_1 = \frac{\mu_{1+}^2 - \mu_{1-}^2}{2(-\tau_1)^{\frac{1}{2}}(-t)^{\frac{1}{2}}}$$

and the amplitude $A(s,\tau_1,z_1,\tau_2,z_2;\ t)$ may be re-expressed in terms of the mass variables and t.

From our approximate solution Eq. (2.43), we have the following prediction of high energy "form factors"

$$\left(\frac{m_0^2}{m_0^2 - \left(\mu^2 - \frac{t}{4}\right)}\right)^{\alpha(t)+1} \quad \text{for } \mu_{1+}^2 = \mu_{1-}^2 = \mu^2, \text{ (Fig. 11a)}, \qquad (4.5a)$$

$$\left(\frac{m_0^2}{m_0^2 - \left(u - \frac{t}{4}\right)}\right)^{\alpha(t)+1} \quad \text{for } \mu_{1+}^2 = \mu_{1-}^2 = u, \text{ (Fig. 11b),} \tag{4.5b}$$

$$\left(\frac{m_0^2}{m_0^2 - \frac{1}{2}\left[\left(\mu^2 - \frac{t}{4}\right) + \left(u - \frac{t}{4}\right)\right]}\right)^{\alpha(t)+1} \quad \text{for } \mu_{1+}^2 = u, \ \mu_{1-}^2 = \mu^2, \text{ (Fig. 11c).} \tag{4.5c}$$

Theoretically, these form factors are important in the following aspects: If later on we want to include the high energy scattering part in σ^{el} in the input, then we can include such off-shell correction so that the Fredholmness of the kernel is maintained. And similarly, when we calculate certain diagrams which correspond to processes involving high energy off-shell scattering, we can include such corrections so that we don't have to use the embarrassing cut-off's in some divergent integrals or to introduce some ad hoc "exponential damping factors."

Phenomenologically, these form factors may give rise to observable effects as well, though it might be difficult to detect that, because high statistics on relatively large momentum transfer events are needed for this purpose. Nevertheless, let us indicate here how this could be done, in principle at least. Consider for example the reaction $\pi^- p \to n\pi^+\pi^-$ (cf. Fig. 12) with the invariant squared mass of the $\pi^+\pi^-$ system above, say, 3 GeV^2. There may not be many events of this type if the pion incident momentum is around 10-20 GeV/c. However, in the future when larger accelerators are in operation, and

thus more phase space opens up, we may then be able to collect many of these events to study high energy π-π scattering via Chew-Low extrapolation. The differential cross for the process stated above is, according to one-pion-exchange model,

$$\frac{d^3\sigma}{duds'dt} = \frac{1}{16\pi^3\Delta(s,\mu^2,M^2)}\,[\pi 2g^2 uF(u)]\,\frac{1}{(u-\mu^2)^2} \times \left[\Delta^{\frac{1}{2}}(s',\mu^2,u)\,\frac{d\sigma_{\pi\pi}^{el}(s',t,u)}{dt}\right], \tag{4.6}$$

where $g^2 = 14.4 \times 4\pi$, and $F(u)$ is the Dürr-Pilkuhn form factor for the left vertex. From another low-energy process $\pi^- p \to n\rho^0$, we know that

$$F(u) = \left(\frac{r_N^{-2} - \mu^2}{r_N^{-2} - u}\right), \quad \text{with } r_N^{-2} \approx 10\mu^2 . \tag{4.7}$$

Our main concern here is, of course, the off-shell elastic cross section of the process $\pi^-(\mu^2) + \pi^+(u) \to \pi^-(\mu^2) + \pi^+(\mu^2)$. In the same spirit as that mentioned in approximation number (2) in the beginning of Sec. III, we use expression (4.5c) and put the "scale factor" $m_0^2 \approx 1$ GeV^2. In order to be easier to compare with experiment, we may write, instead of Eq. (4.6),

$$\frac{d\sigma}{du} \approx \frac{1}{16\pi^3\Delta(s,\mu^2,M^2)}\,[\pi 2g^2 uF(u)]\,\frac{1}{(u-\mu^2)^2} \times \left[\int_3^{s'_{max}(s,u)} ds'\ \Delta^{\frac{1}{2}}(s',\mu^2,u)\ \sigma_{\pi\pi}^{el}(s')\ \mathcal{F}(u)\right], \tag{4.8}$$

where $\sigma^{el}(s')$ is the on-shell cross section

$$\mathcal{F}(u) = \left(\frac{m_0^2}{m_0^2 - \frac{1}{2}(\mu^2 + u)} \right)^{2\alpha(0)+2}, \quad \text{with } m_0^2 \approx 1 \text{ GeV}^2, \quad (4.9)$$

and $\alpha(0)$ is the intercept of the highest Regge trajectory in $\sigma^{el}_{\pi\pi}(s')$. In deriving Eq. (4.8) from Eq. (4.6) we have made use of the presumption that $d\sigma^{el}_{\pi\pi}/dt$ has a sharp forward peak.

Note, for example, that when $u = -0.4$ GeV^2, $\mathcal{F}(u) = 0.5$ for $\alpha(0) = 1$. Thus the predictions for the differential cross section at this momentum transfer differ by a factor of 2 when Eq. (4.8) is used with or without the form factor Eq. (4.9).

On the other hand, we may choose a value of m_0^2 to give the best fit to data. Then the precise value of $d\sigma^{el}_{\pi\pi}/dt$ (Thus $\sigma^{tot}_{\pi\pi}$ via optical theorem) deduced from extrapolation with Eq. (4.6) from experiment can help us to prove the factorization properties of the Pomeranchukon.

V. INCLUSION OF THE HIGH ENERGY TAIL IN THE KERNEL

In this section we shall discuss, for completeness, an attempt to include the high energy scattering part in the potential V. To be specific, we shall keep on working on the simplified version of the model outlined in Sec. III, and use Eq. (2.16) or Eq. (2.43) as the solution when V contains the low energy resonance part only. There are a number of reasons for the desire to make improvement on this kind of solution. Let us state some of them. Quantitatively: the output values (include those obtained from realistic and accurate numerical studies[2,18,19]) for $\alpha(0)$, $\alpha'(0)$, β_α, etc. are not in excellent agreement with experiments or expectations. Qualitatively: (i) there is no reason why V, the basic building block in the multi-peripheral chain, should not contain the high energy scattering part, (ii) a complete scheme should have the Froissart bound built in, and (iii) phenomenologically, it is well known that pure (real) pole amplitudes, either in the vacuum or nonvacuum crossed channel, can not explain all the aspects of high energy data.

The particular method[3] we use to implement the improvement goes through the following steps.

(1) Let an energy s_0^* be chosen such that, to a good approximation, we may describe V with resonances only (call it V^R) for $s_0 < s_0^*$, with high energy (diffractive) scattering only (call it V^P) for $s \geq s_0^*$.

(2) When $V = V^R$ alone, accept that the solution is given by Eq. (2.16) or Eq. (2.43) (together with a signature factor for the full amplitude if needed). Thus

$$\frac{A_\lambda^R}{(-\tau_1)^{\frac{\lambda+1}{2}}\,(-\tau_2)^{\frac{\lambda+1}{2}}} = \frac{\tilde{b}_\lambda(\tau_1,t)\,\tilde{b}_\lambda(\tau_2,t)}{\lambda - \alpha_R} \quad , \tag{5.1}$$

$$A^R = \tilde{b}_{\alpha_R}(\tau_1,t)\,\tilde{b}_{\alpha_R}(\tau_2,t)\left(\frac{s}{m_0^2}\right)^{\alpha_R} \quad , \tag{5.2}$$

where α_R is assumed to be "quite close" to 1,

$$\tilde{b}_\lambda(\tau,t) = [\bar{\beta}_{\alpha_R}(t)]^{\frac{1}{2}}\left(\frac{m_0^2}{m_0^2 - \tau}\right)^{\lambda+1} \quad , \tag{5.3}$$

$$\tilde{b}_{\alpha_R}(\tau,t) = [\bar{\beta}_{\alpha_R}(t)]^{\frac{1}{2}}\left(\frac{m_0^2}{m_0^2 - \tau}\right)^{\alpha_R+1} \quad , \tag{5.4}$$

$$\bar{\beta}_{\alpha_R} = 16\pi^3\,\beta_{\alpha_R} \quad , \tag{5.5}$$

and we have dropped the symmetry index $I_t = 1$ for the moment.

(3) Guess that the leading behavior of the <u>final</u> amplitude is again Regge-pole behaved

$$T = b_\alpha(\tau_1,t)\,b_\alpha(\tau_2,t)\left(\frac{s}{m_0^2}\right)^{\alpha} \quad , \tag{5.6}$$

where

$$b_\alpha(\tau,t) = \left[\left(i - \operatorname{ctn}\frac{\pi\alpha}{2}\right)\bar{\beta}_\alpha(t)\right]^{\frac{1}{2}}\left(\frac{m_0^2}{m_0^2 - \tau}\right)^{\alpha+1} \quad , \tag{5.7}$$

where α, $\bar{\beta}_\alpha$ are supposed to be calculated. We may conveniently parametrize $\bar{\beta}_\alpha(t)$ by

$$\bar{\beta}_\alpha(t) = \bar{\beta}_\alpha(0)\,e^{\gamma t} \quad , \tag{5.8}$$

with a constant γ. This form is suggested by experiments.

With this T, we compute V^p with Eq. (2.2), and thus V_λ^p with Eq. (2.3); for $t = 0$

$$V_\lambda^p(0) = \frac{1}{16\pi N_\mu}\int_{-\infty}^{0} dt'(-\tau_1)^{\frac{\lambda+1}{2}}\,(-\tau_2)^{\frac{\lambda+1}{2}}\,|b_\alpha(\tau_1,t')|^2$$

$$\times\ |b_\alpha(\tau_2,t')|^2\ \frac{(s^*)^{-(\lambda-2\alpha(t')+1)}}{\lambda - 2\alpha(t') + 1} \quad . \tag{5.9}$$

This corresponds to a branch cut with branch point $\alpha_c = 2\alpha(0) - 1$ in the λ-plane. Using Eq. (5.7) and Eq. (4.5c), we may write approximately

$$V_\lambda^p(0) \approx \frac{1}{16\pi N_\mu}(-u_1)^{\frac{\lambda+1}{2}}\,(-u_2)^{\frac{\lambda+1}{2}}\left(\frac{m_0^2}{m_0^2 - \frac{1}{2}u_1}\right)^{2\alpha(0)+2}$$

$$\times\left(\frac{m_0^2}{m_0^2 - \frac{1}{2}u_2}\right)^{2\alpha(0)+2}\frac{|\bar{\beta}_\alpha(0)|^2}{2\alpha'(0)}\,E_1\left(\left(\frac{\gamma}{\alpha'(0)} + \ell n\ s^*\right)(\lambda - \alpha_c)\right) \quad , \tag{5.10}$$

where $\alpha'(0)$ is the derivative of $\alpha(t)$ at $t = 0$, and E_1 is the Exponential Integral.

Reasonable estimates[2] show that

$$V_\lambda^R \gg V_\lambda^P \tag{5.11}$$

for λ not too close to the tip of the branch cut.

(4) Now treat Eq. (5.1) as the "unperturbed" solution to the problem. With the additional "small" piece V_λ^P in V_λ, we may calculate[29] the "perturbed" solution by the variational principle of Schwinger. The forward partial-wave amplitude is then given by

$$\frac{A_\lambda}{(-\tau_1)^{\frac{\lambda+1}{2}}(-\tau_2)^{\frac{\lambda+1}{2}}} \sim \kappa_\lambda \kappa_\lambda' \tilde{b}_\lambda \tilde{b}_\lambda + \frac{\kappa_\lambda^2 \tilde{b}_\lambda \tilde{b}_\lambda + \kappa_\lambda \epsilon_\lambda (\tilde{b}_\lambda |b_\alpha|^2 + |b_\alpha|^2 \tilde{b}_\lambda) E_1 + \eta_\lambda^{-1} \epsilon_\lambda^2 (\lambda - \alpha_R) |b_\alpha|^2 |b_\alpha|^2 E_1}{\lambda - \alpha_R - \eta_\lambda E_1}, \tag{5.12}$$

where

$$\tilde{b}_\lambda |b_\alpha|^2 \equiv \tilde{b}_\lambda(\tau_1,0) |b_\alpha(\tau_2,0)|^2, \text{ etc.,} \tag{5.13}$$

$$\kappa_\lambda = \mathrm{Tr}\, K_\lambda \approx 1 - \kappa_\lambda'(\lambda - \alpha_R), \tag{5.14}$$

$$\kappa_\lambda' = \frac{R(0)}{16\pi^3 \beta_{\alpha_R}(0)}, \tag{5.15}$$

$$\epsilon_\lambda = \left[\frac{\eta_\lambda}{16\pi\, 2\alpha'(0)}\right]^{\frac{1}{2}}, \tag{5.16}$$

$$\eta_\lambda = \frac{1}{16\pi\, 2\alpha'(0)} G_\lambda^2(0)\, e^{\frac{\gamma}{\alpha'(0)}(\lambda - \alpha_c)}, \tag{5.17}$$

and the triple-Pomeranchukon coupling[30]

$$G_\lambda(0) = \frac{1}{16\pi^3 N_\mu^{\frac{1}{2}}(\lambda+1)} \int_{-\infty}^{0} d\tau' \frac{(-\tau')^{\lambda+1}}{(\tau')^2} |b_\alpha(\tau',0)|^2 \tilde{b}_\lambda(\tau',0) \tag{5.18}$$

$$= \frac{1}{16\pi^3 N_\mu^{\frac{1}{2}}(\lambda+1)} \bar{\beta}_\alpha(0)\, \bar{\beta}_{\alpha_R}^{\frac{1}{2}}(0) (2)^{2\alpha(0)+2}$$

$$\times\ B\big(2\alpha(0)+3, \lambda\big)\, F\big(2\alpha(0)+2,\ 2\alpha(0)+3,\ 2\alpha(0)+3+\lambda, -1\big)\ . \tag{5.19}$$

Expression (5.12) has a branch cut in the λ-plane starting at $\alpha_c = 2\alpha(0) - 1$. We shall draw this cut to the left along the real axis from α_c to $-\infty$.

Part of the <u>self-consistency requirements</u> on Eq. (5.12) is to identify the <u>l</u>st sheet zero of the denominator (there is only one such zero and it is real) with α and the corresponding residue with $\tilde{b}_\alpha \tilde{b}_\alpha$. It can be shown that, for $\alpha_R < \alpha_c$, this zero lies above α_c but below 1.[31] (A physically acceptable solution must, of course, have α just slightly below 1.) When Eq. (5.12) is transformed back to the physical s-plane, we pick up the pole and the discontinuity across the cut:

$$A \sim \tilde{b}_\alpha \tilde{b}_\alpha \left(\frac{s}{m_0^2}\right)^\alpha + \int_{-\infty}^{\alpha_c} d\lambda \left(\frac{s}{m_0^2}\right)^\lambda \mathrm{disc}\, A_\lambda\ , \tag{5.20}$$

where $\tilde{b}_\alpha \tilde{b}_\alpha$, the residue of the pole, can be computed from Eq. (5.12), and

$$\text{disc } A_\lambda = \frac{[\kappa_\lambda \eta_\lambda^{\frac{1}{2}} \tilde{b}_\lambda + \eta_\lambda^{-\frac{1}{2}} \epsilon_\lambda (\lambda - \alpha_R) |b_\alpha|^2][\eta_\lambda^{-\frac{1}{2}} \epsilon_\lambda (\lambda - \alpha_R) |b_\alpha|^2 + \kappa_\lambda \eta_\lambda^{\frac{1}{2}} \tilde{b}_\lambda]}{(\lambda - \alpha_R - \eta_\lambda |E_1|)^2 + \pi^2 \eta_\lambda^2} , \tag{5.21}$$

where the first bracket has argument τ_1, the second has τ_2.

We close by pointing out some qualitative properties of this solution:[32]

(1) As we have mentioned, the leading pole is real and closer (than α_R) to 1 but never exceeds 1.

(2) The residue $\tilde{b}_\alpha \tilde{b}_\alpha$ is smaller than $\tilde{b}_{\alpha_R} \tilde{b}_{\alpha_R}$.

(3) The off-shell behavior of this pole is just

$$\left(\frac{m_0^2}{m_0^2 - \tau_1}\right)^{\alpha+1} \left(\frac{m_0^2}{m_0^2 - \tau_2}\right)^{\alpha+1} .$$

(4) The discontinuity disc A_λ is always positive when all the legs of A_λ are on-shell. And disc $A_\lambda \to 0$ as $\lambda \to \alpha_c$. [Note, however, that the condition Eq. (5.11) does not hold in this limit.] The cut integral may be associated with secondary Regge singularities.

ACKNOWLEDGMENTS

I am most grateful to Professor Geoffrey F. Chew for teaching me physics (and sometimes nonacademic matters) throughout my graduate years. His continuing inspiration and guidance are deeply appreciated.

The observation about cross section data reported in Sec. I came from discussions with H. J. Yesian. It was a great pleasure to collaborate with B. R. Webber in the work reported in Sec. II. The work reported in Sec. III began by the stimulating discussions with S. S. Shei, and I benefited from comments on this work from Professor J. David Jackson and C. Sorensen. I had some helpful conversations with D. Lissauer about the work reported in Sec. IV. Some of the results reported in Sec. V have been derived independently by C. Sorensen.

I thank my friends Chi Sum Lui and Herbert W. T. Yim for their encouragements some years ago.

There will be no acknowledgment here to Mei-Mei Chan. If I want to thank her, I shall whisper to her.

FOOTNOTES AND REFERENCES

* This work was supported by the U. S. Atomic Energy Commission.

1. L. Bertocchi, S. Fubini, and M. Tonin, Nuovo Cimento 25, 626 (1962); D. Amati, A. Stanghellini, and S. Fubini, ibid. 26, 6 (1962).

2. G. F. Chew, T. Rogers, and D. Snider, Phys. Rev. D2, 765 (1970).

3. H. D. I. Abarbanel, G. F. Chew, M. L. Goldberger, and L. M. Saunders, Princeton Preprint (March 1971) and references therein.

4. Compilation of Cross Sections III--K^+ Induced Reactions, CERN/HERA 70-4 (Sept. 1970), and A Compilation of K^+N Reactions, Lawrence Radiation Laboratory Report UCRL-20000 (Sept. 1969).

5. In the second paper of Ref. 1.

6. D. Silverman and P. D. Ting, University of California, San Diego preprint UCSD-10P10-82 (1971).

7. H. D. I. Abarbanel, G. F. Chew, M. L. Goldberger, and L. M. Saunders, Phys. Rev. Letters 25, 1735 (1970).

8. J. Dash, Cambridge preprints DAMTP 71/12 (April 1971), DAMTP 71/19 (May 1971).

9. L. M. Saunders, O. H. N. Saxton, and C. I. Tan, Phys. Rev. D3, 1005 (1971).

10. It can be shown, from Eq. (2.50) below and the properties of Gegenbauer polynomials, that higher terms in Eq. (2.28) affect the trajectories determined by Eq. (2.29) only to the order t^2 and higher. A similar conclusion was obtained by V. Chung and D. Snider [Phys. Rev. 162, 1639 (1967)], and M. L. Goldberger, Princeton University (private communication to G. F. Chew, June, 1971).

11. See, for example: W. Magnus, F. Oberhettinger, and R. P. Soni, Formulas and Theorems for the Special Functions of Mathematical Physics, Die Grundlehren der Mathematischen Wisenschaften in Einzeldarstellungen, Band 52 (Springer-Verlag, New York, Inc., 1966). The formula we needed is

$$F(a,b,c,1-x) = \frac{\Gamma(c)\Gamma(c-a-b)}{\Gamma(c-b)\Gamma(c-a)} F(a,b,a+b-c+1,x)$$

$$+ x^{c-a-b} \frac{\Gamma(c)\Gamma(a+b-c)}{\Gamma(a)\Gamma(b)} F(c-a,\, c-b,\, c-a-b+1,\, x),$$

for $|\arg x| < \pi$. When $c - a - b = \pm 0, \pm 1, \pm 2, \cdots$, this expression is still valid but we must pass to the limit with care, e.g.,

$$F(a,b,a+b+k,\, 1-x)$$

$$= \frac{\Gamma(k)\Gamma(a+b+k)}{\Gamma(a+k)\Gamma(b+k)} \sum_{n=0}^{k-1} \frac{\Gamma(a+n)\Gamma(b+n)}{\Gamma(a)\Gamma(b)} \frac{\Gamma(1-k)}{\Gamma(1-k+n)} \frac{x^n}{n!}$$

$$- \frac{\Gamma(a+b+k)}{\Gamma(a)\Gamma(b)} x^k \sum_{n=0}^{\infty} \frac{\Gamma(a+k+n)\Gamma(b+k+n)}{\Gamma(a+k)\Gamma(b+k)} \frac{x^n}{n!(k+n)!}$$

$$\times [\log x - \psi(n+1) + \psi(a+k+n) + \psi(b+k+n)$$

$$- \psi(1+k+n)]$$

for $|\arg x| < \pi$, $|x| < 1$, $k = 1,2,3,\cdots$. This gives, for example, Eq. (2.33) below when $\zeta = 0$ and $\ell \to 1$,

$$1 = \frac{R(0)}{16\pi^3}\left\{\frac{1}{6} + \left(\log\frac{\mu^2}{m^2} + \frac{7}{3}\right)\left(\frac{\mu^2}{m^2}\right) + 6\left(\log\frac{\mu^2}{m^2} + \frac{17}{12}\right)\left(\frac{\mu^2}{m^2}\right)^2 + \cdots\right\}.$$

12. H. W. Wyld, Jr., Phys. Rev. D3, 3090 (1971).

13. We computed the slope to order $[(\mu^2)/(m^2)]^2$ because the series X in Eq. (2.37) and Y in Eq. (2.40) converge less rapidly than that in Eq. (2.33). Although the $O\{[(\mu^2)/(m^2)]^2\}$ terms are in magnitude only about 15% of the $O(1) + O[(\mu^2)/(m^2)]$ terms, they contribute with opposite signs to X and Y, making the quotient X/Y change by about 30%.

14. G. Tiktopoulos and S. B. Treiman, Phys. Rev 137, 1597 (1965).

15. Our approximate solution shown in Fig. 3 lies slightly above the exact solution for $\alpha(0) \lesssim 1/3$. This is due to the fact that we have computed $\alpha(0)$ from Eq. (2.33) only up to first order in $[(\mu^2)/(m^2)]$. Inclusion of higher order $[(\mu^2)/(m^2)]$ terms will make it lie below the exact solution in that region also.

16. This section is based on the paper by C. F. Chan and B. R. Webber, Phys. Rev. D5, 933 (1972).

17. This section is based on the paper by C. F. Chan, Phys. Rev. D4, 3466 (1971).

18. D. M. Tow, Phys. Rev. D2, 154 (1970).

19. D. Avalos and B. R. Webber, Phys. Rev. D4, 3313 (1971).

20. Our conventions:

$$S = 1 + i(2\pi)^4 \delta^4(P_f - p_i)T .$$

The phase space factor $d^3p/(2\pi)^3 2E_p$ is used for both bosons and fermions. For μB scattering, we have

$$T_{\mu B} = \bar{u}(\mathcal{A} + \gamma\cdot Q\mathcal{B})u ,$$

with $(\gamma\cdot p - M)\, u(p) = 0$ and $\bar{u}u = 2M$.

$$A_{\mu B}(s,0) \equiv \mathrm{Im}\, T_{\mu B}(s,0) \sim 2M\, \mathrm{Im}\, \mathcal{A}(s,0) + s\, \mathrm{Im}\, \mathcal{B}(s,0).$$

The μ-B-B vertex is given by

$$T_{\mu B} = iG\bar{u}\gamma_5\tau_i u \qquad \text{for SU(2) model, and}$$

$$T_{\mu B} = i\alpha G\bar{u}\gamma_5 2D_i u + i(1-\alpha)G\bar{u}\gamma_5 2F_i u \qquad \text{for SU(3) model.}$$

When μ = pion, B = nucleon, and all the three particles are on-shell, $G^2 = g^2 \approx 14.4 \times 4\pi$.

21. H. P. Dürr and H. Pilkuhn, Nuovo Cimento 40, 899 (1965).

22. D. Amati, L. L. Foldy, A. Stanghellini, and L. Van Hove, Nuovo Cimento 32, 1686 (1964).

23. For example, $M = M_0 + M_1 Y + M_2[2 - 2I(I+1) + \frac{1}{2}Y^2]$ for B_8, such an assignment of M_0 as the mass in the "exact symmetry limit" is not unambiguous.

24. The "radius" r is expected to be roughly equal to the Compton wavelength of the lightest particle that μ and B can exchange. A value of r^{-2} ranging from $5\mu^2$ to $20\mu^2$ (the precise choice is not critically important) is used in most data fittings for singly peripheral reactions. In our case, the value of the integral in Eq. (3.7) is not sensitive to our particular choice of $r^{-2} = \frac{1}{2}m_0^2$, since the form factor $r^{-2}/(r^{-2} - \tau')$ is close to unity in the small τ' region where the integrand contributes most to the integral, the tail of the integrand (with the factor $\sim r^{-2}/\tau'$) not contributing much. In fact it can be shown that if we change r^{-2} by $\pm 50\%$ relative to the choice above, then the value of the integrals changes only $\pm 10\%$.

25. In the sense of R. E. Cutkosky, Ann. Phys. 23, 415 (1963); R. H. Capps, Nuovo Cimento 27, 1208 (1963); A. W. Martin and K. C. Wali, Phys. Rev. 130, 2455 (1963), Nuovo Cimento 31, 1324 (1964). The static model is, of course, consistent with our neglect of the μ mass here. On the other hand, if we take the mass formulas seriously, then $\mu = 0.412$ GeV and thus R lies below the (μB) threshold in the "exact symmetry limit." This was noted by R. J. Oakes and C. N. Yang, Phys. Rev. Letters 11, 174 (1963). In any case, we may defend the plausibility of the width Γ_R calculated here as corresponding to the most commonly observed magnitude of (μB) resonance widths. Furthermore the value of the factor $\pi\, m_R\, \Gamma_R\, \sigma^R(\max)$ computed in our way turns out to be nearly the same as that computed from the observed values of the corresponding quantities for $\Delta(1236)$. Therefore it seems likely that we have not underestimated this factor in the (μB) resonance contribution.

26. From our choice of the values of α and g^2, and using the observed masses and phase space, the calculated width of $\Delta(1236)$ is $\Gamma_{\Delta \to N\pi} \approx 0.1$ GeV. The decay channl $\Delta \to \Sigma K$, which represents half of the total decay probability with SU(3) symmetry, is closed.

27. J. V. Allaby et al., Phys. Letters 30B, 500 (1969).

28. V. Barger et al., Nucl. Phys. B5, 411 (1968), or Barger and Cline, Phenomenological Theories of High Energy Scattering (W. A. Benjamin, Inc. Publishers, New York, 1969).

29. With the factorizable approximation for $V_\lambda^{\ p}$ given by Eq. (5.10), we may alternatively solve the equation with Eq. (2.52). But the method presented is good even if we don't use the factorizable form for $V_\lambda^{\ p}$.

30. If $m_0^{\ 2} = 1$ GeV^2, $\alpha_R = 0.8$, $\lambda = \alpha = 1$ (it does not matter for α to be arbitrary close to 1 here), $N_\mu = 8$ and $\sigma_{\mu\mu}^{tot} \sim |\tilde{b}_\alpha|^2/N_\mu \sim 15$ mb, then $G_1(0) = 0.81$ GeV^{-1}. Thus $\eta = 0.016$ if $\alpha'(0) = 0.4$.

31. S. S. Shei, Phys. Rev. D4, 3704 (1971).

32. Further physical implications of this type of solution have been discussed (in a more general way) by G. F. Chew and D. R. Snider, preprint NAL-THY-53 (May 1972).

Table I. The variables.

$$s = (p_1 - p_2)^2$$

$$t = q^2$$

$$\cosh\theta = \frac{-p_1\cdot p_2}{(-\tau_1)^{\frac{1}{2}}(-\tau_2)^{\frac{1}{2}}} = \frac{s - \tau_1 - \tau_2}{2(-\tau_1)^{\frac{1}{2}}(-\tau_2)^{\frac{1}{2}}}$$

$$\tau_1 = p_1^2 \qquad z_1 = \frac{p_1\cdot q}{(-\tau_1)^{\frac{1}{2}}(-t)^{\frac{1}{2}}}$$

$$\tau_2 = p_2^2 \qquad z_2 = \frac{p_2\cdot q}{(-\tau_2)^{\frac{1}{2}}(-t)^{\frac{1}{2}}}$$

$$\tau' = p'^2 \qquad z' = \frac{p'\cdot q}{(-\tau')^{\frac{1}{2}}(-t)^{\frac{1}{2}}}$$

$$-1 \leq z \leq 1 \quad \text{for all } z\text{'s}$$

$$\cosh\psi = \frac{\cosh\theta - z_1 z_2}{(1 - z_1^2)^{\frac{1}{2}}(1 - z_2^2)^{\frac{1}{2}}} .$$

FIGURE CAPTIONS

Fig. 1. Sketch of the total cross section and some individual production cross sections in K^+p scattering. In this figure $\sigma_{K^+p\to K\pi N}$ stands for the sum of σ's of all possible final charge states.

Fig. 2. The kinematic structure of the multiperipheral integral equation.

Fig. 3. Solutions for the intercept of the leading pole when $\mu^2 = 0$.

Fig. 4. Solutions for the intercept of the leading pole when $\mu^2 = m_\pi^2$.

Fig. 5. Solutions for the residue of the leading pole when $\mu^2 = 0$.

Fig. 6. Solutions for the residue of the leading pole when $\mu^2 = m_\pi^2$.

Fig. 7. Off-shell dependence of the residue of the leading pole when $\mu^2 = 0$. The exact numerical solutions are shown in heavy lines, whereas $\phi_\alpha(\tau_1,0)$ calculated from Eq. (2.47) are shown in light lines. Curve I: $\alpha(0) = 1$, $\frac{R(0)}{16\pi^3} = 4.95$. Curve II: $\alpha(0) = 1$, $\frac{R(0)}{16\pi^3} = 6$. Curve III: $\alpha(0) = 0.94$, $\frac{R(0)}{16\pi^3} = 4.95$. Curves 1 and 2: $\alpha(0) = 0.7$, $\frac{R(0)}{16\pi^3} \approx 2.5$.

Fig. 8. Slope of the leading pole at $t = 0$.

Fig. 9. Production amplitude of μB scattering of (a) even numbers of final μ's and (b) odd numbers of final μ's.

Fig. 10. Schematic representation of $\sigma_{\pi N}$'s.

Fig. 11. The high energy vertices when (a) both legs on-shell [Eq. (4.5a)], (b) one leg on-shell, one leg off-shell [Eq. (4.5b)], and (c) both legs off-shell [Eq. (4.5c)].

Fig. 12. The process $\pi^-p \to \pi^-\pi^+n$.

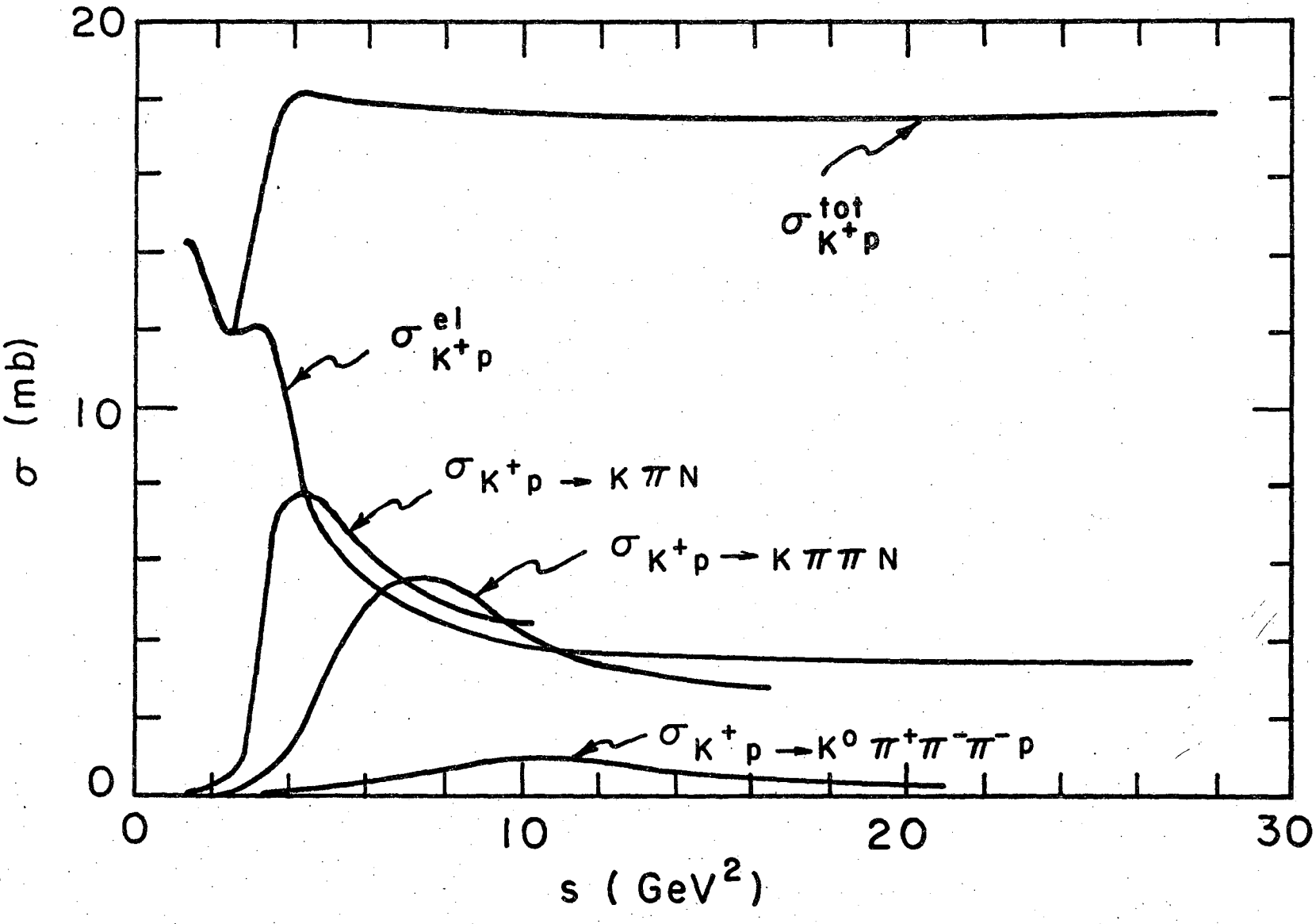

XBL728-3797

Fig. 1.

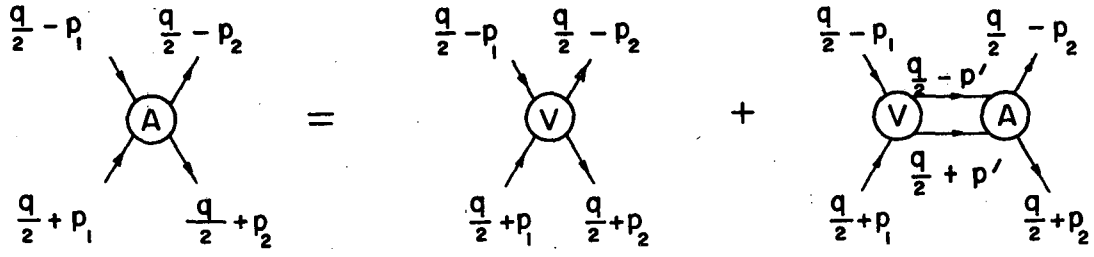

XBL719-4376

Fig. 2.

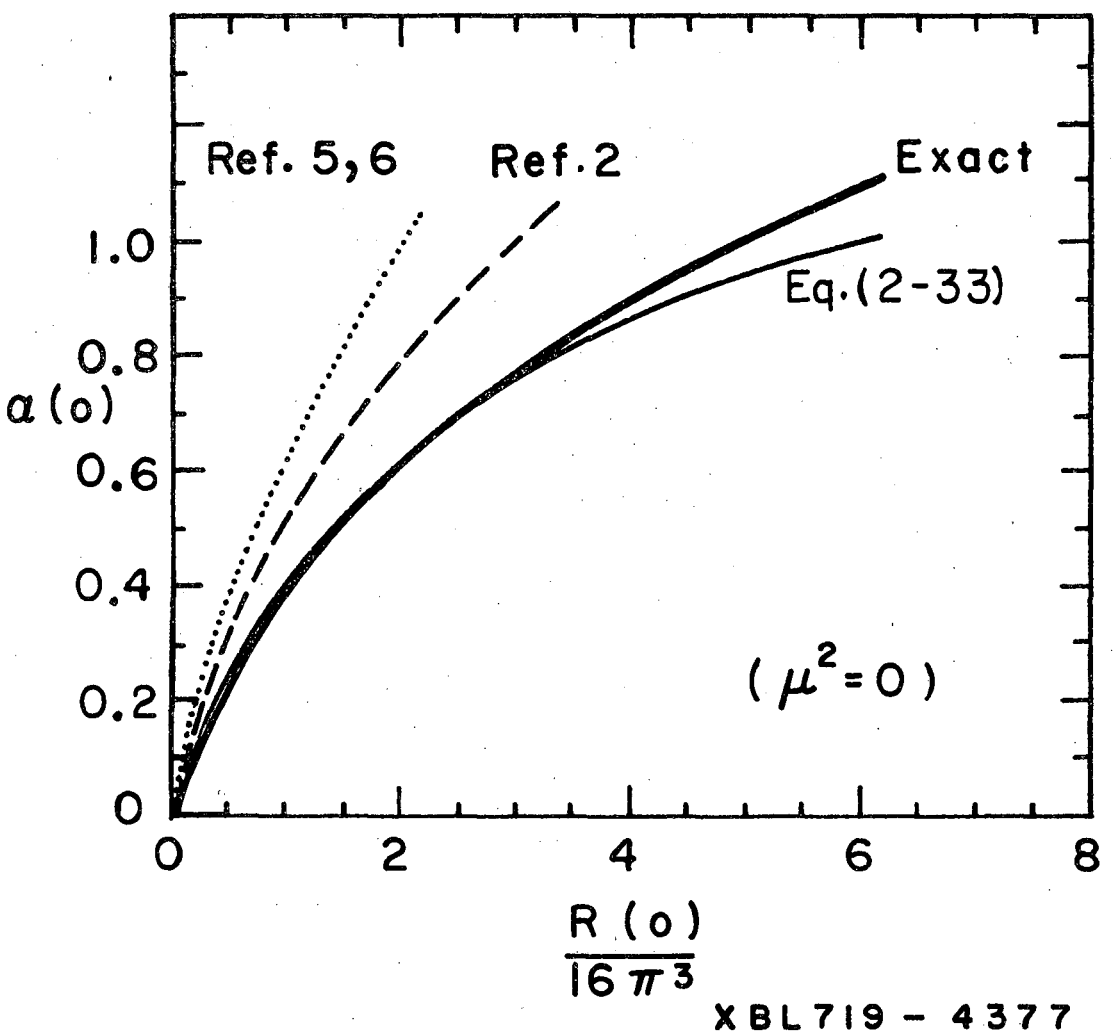

Fig. 3.

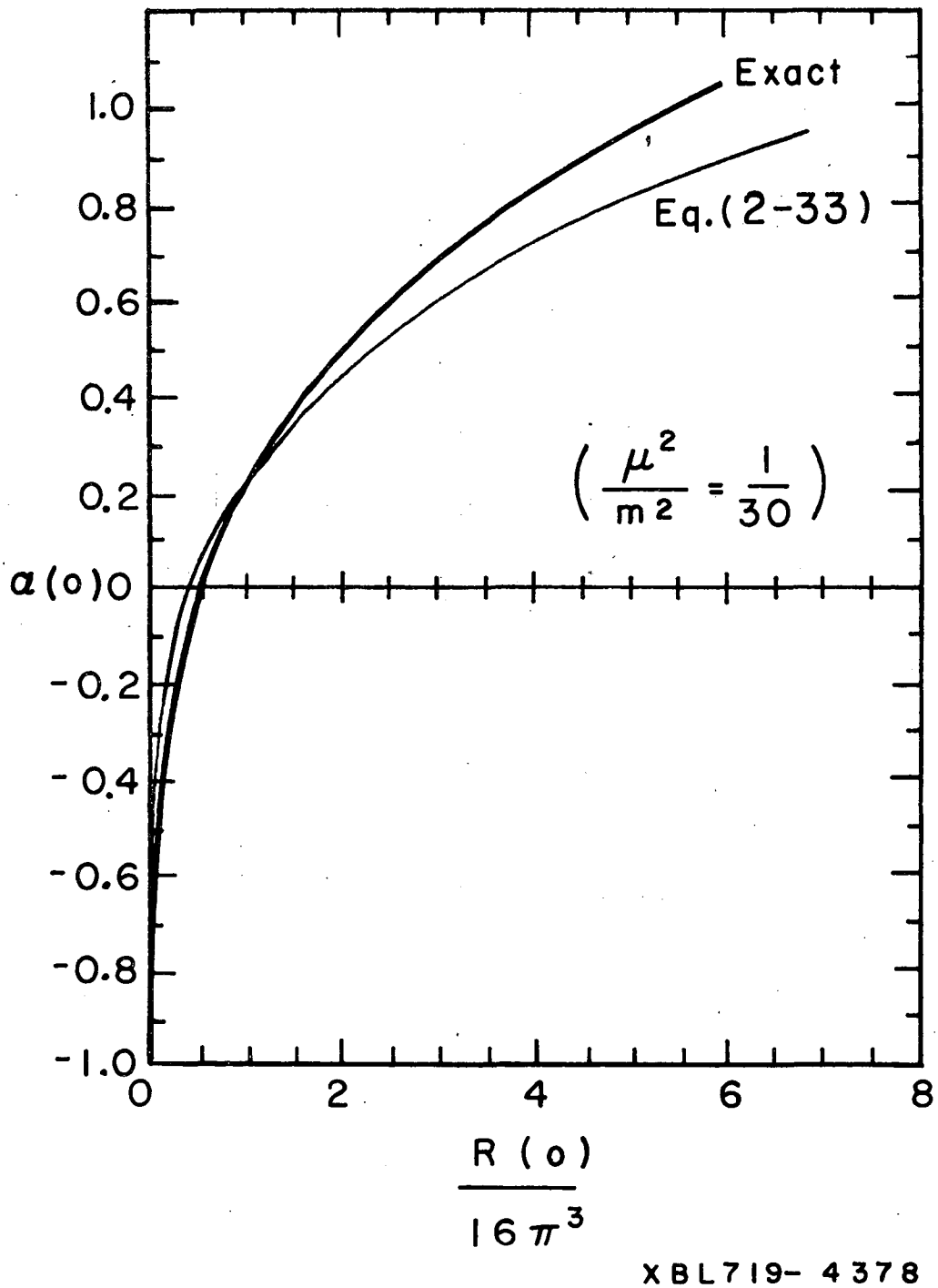
Exact
Eq.(2-33)
$\left(\frac{\mu^2}{m^2} = \frac{1}{30}\right)$
1.0
0.8
0.6
0.4
0.2
α(o)0
-0.2
-0.4
-0.6
-0.8
-1.0
0
2
4
6
8
$\frac{R(o)}{16\pi^3}$
XBL719-4378

Fig. 4.

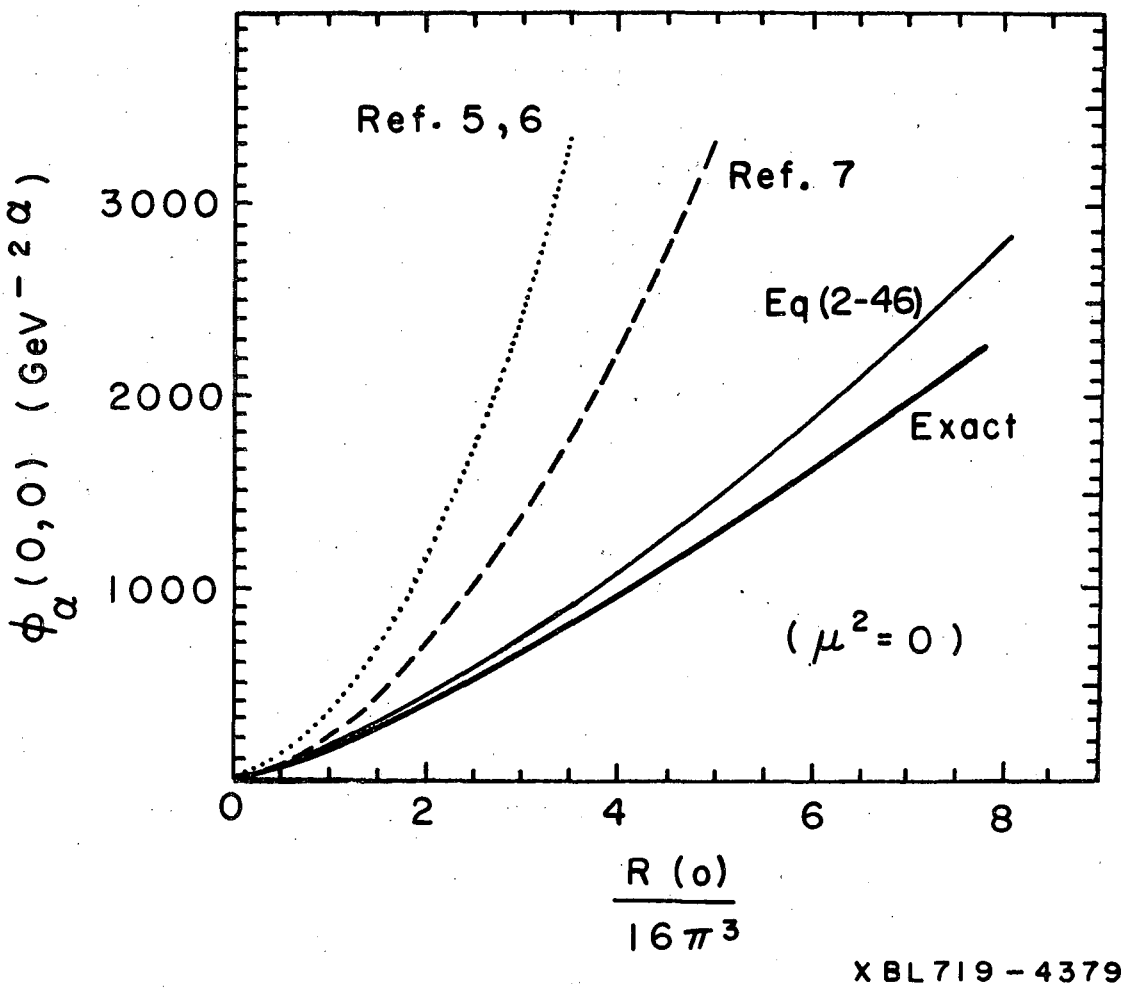
Ref. 5,6
Ref. 7
Eq (2-46)
Exact
$(\mu^2 = 0)$
$\phi_\alpha(0,0)$ (GeV$^{-2\alpha}$)
3000
2000
1000
0
2
4
6
8
$\frac{R(o)}{16\pi^3}$
XBL719-4379

Fig. 5.

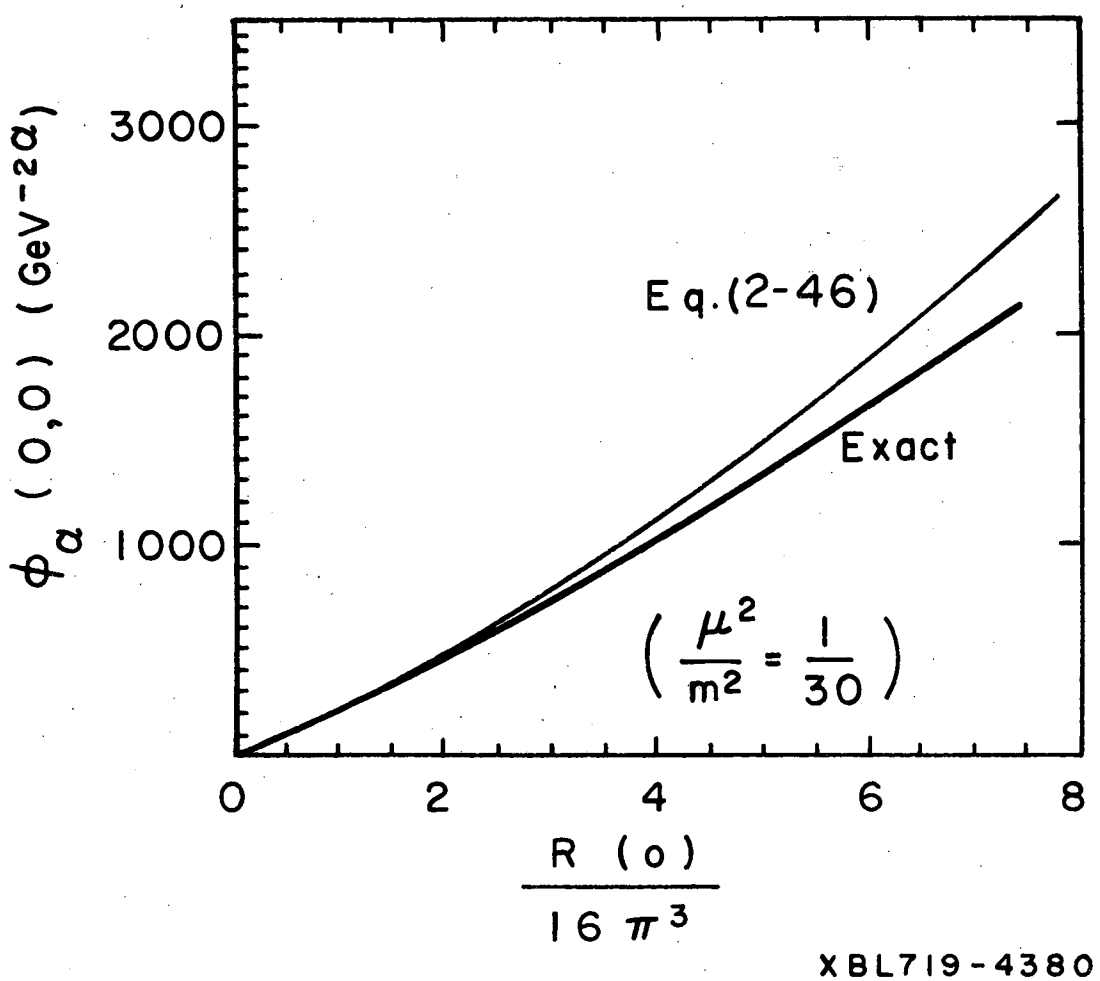
ϕ_a (0,0) (GeV^{-2a})
3000
2000
1000
0
2
4
6
8
Eq.(2-46)
Exact
$\left(\frac{\mu^2}{m^2} = \frac{1}{30}\right)$
$\frac{R\ (o)}{16\ \pi^3}$
XBL719-4380

Fig. 6.

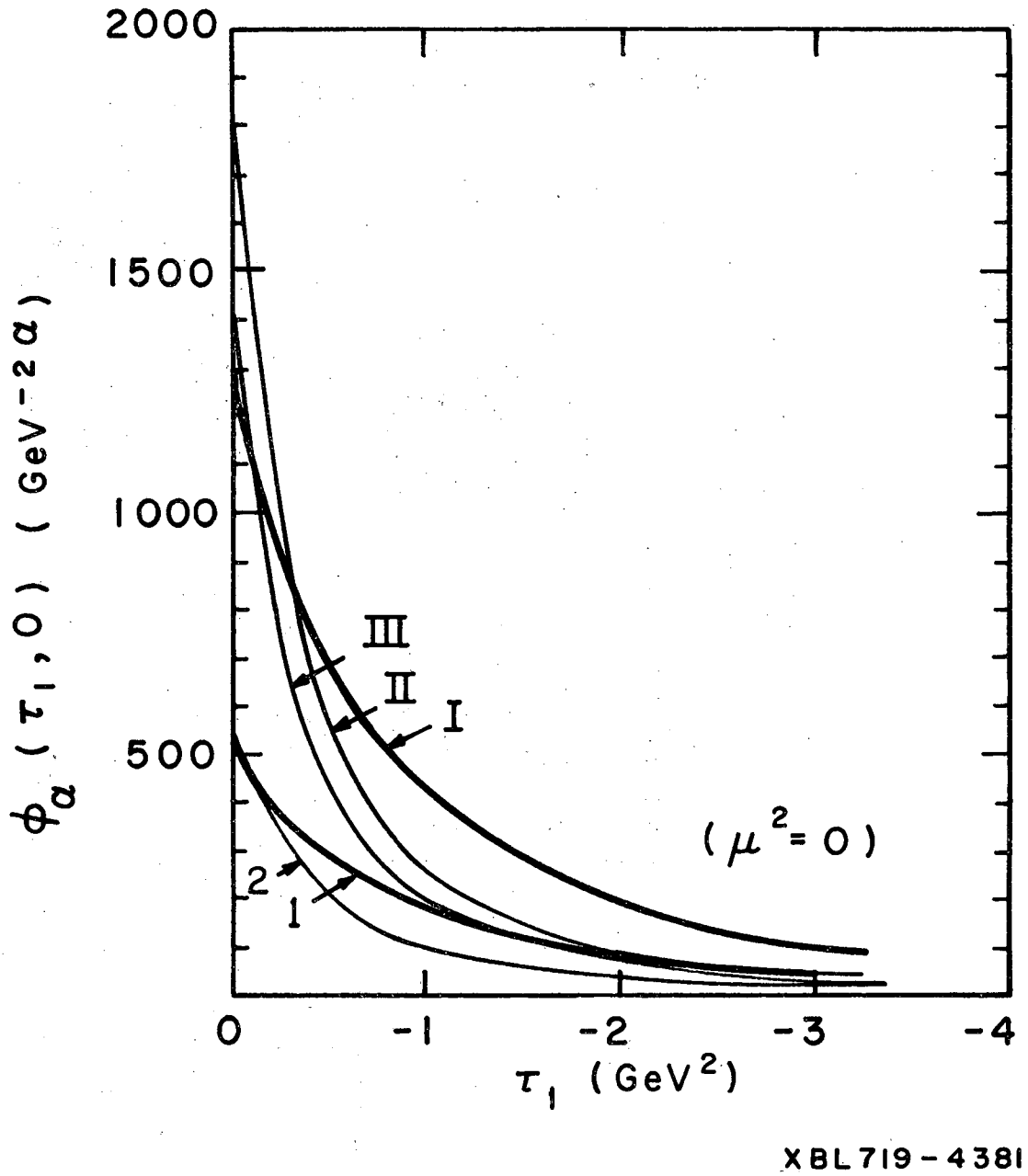
2000
1500
1000
500
0
-1
-2
-3
-4
$\phi_\alpha(\tau_1, 0)$ (GeV$^{-2\alpha}$)
τ_1 (GeV^2)
III
II
I
2
1
($\mu^2 = 0$)
XBL719-4381

Fig. 7.

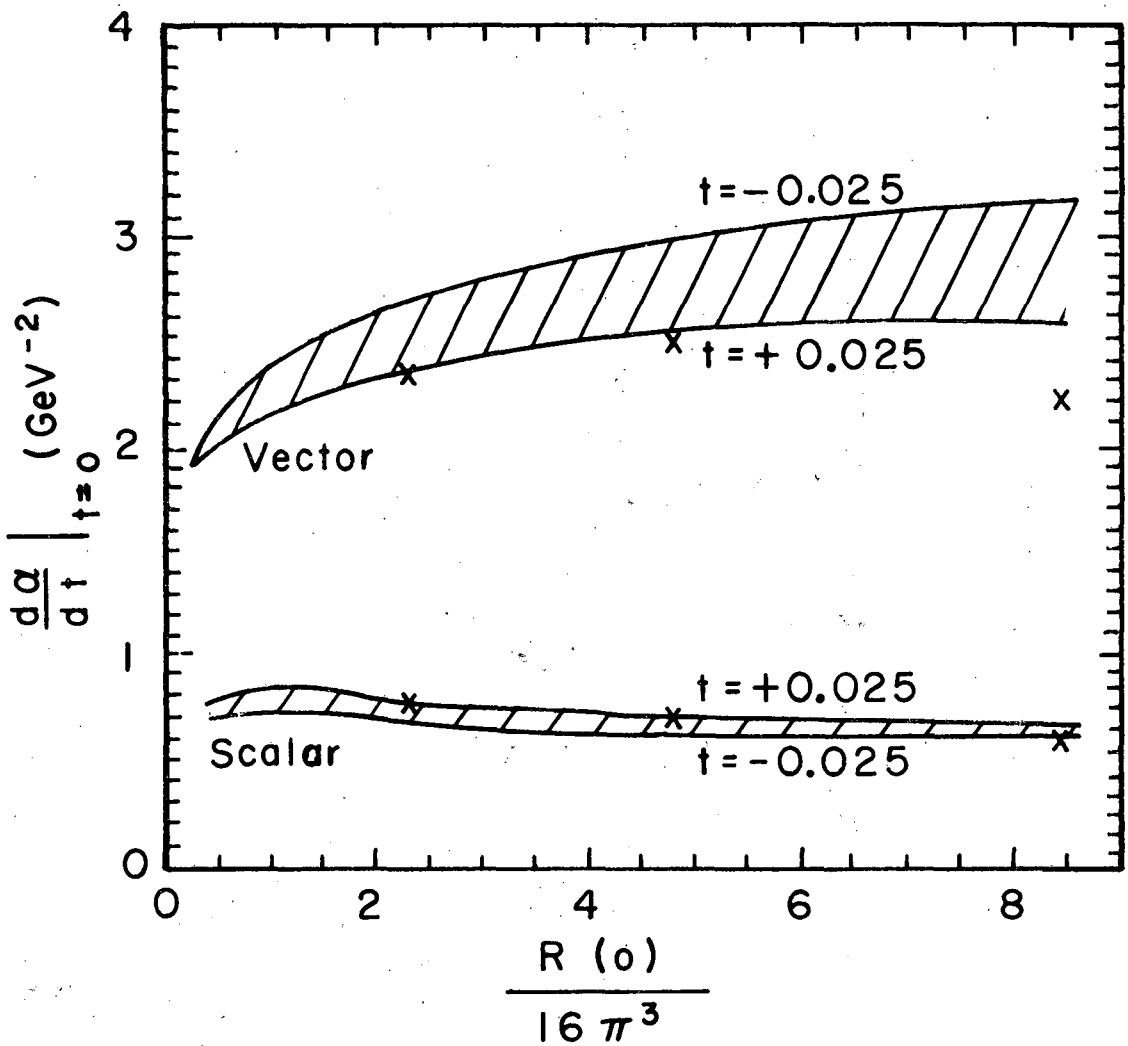

XBL719-4382

Fig. 8.

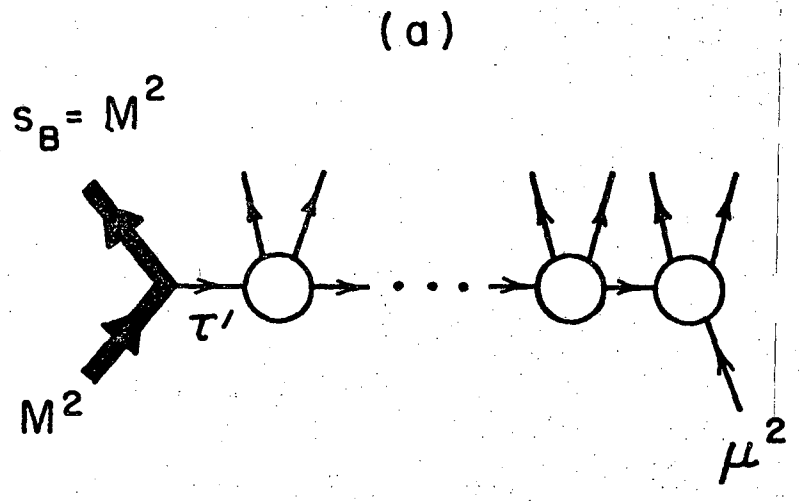

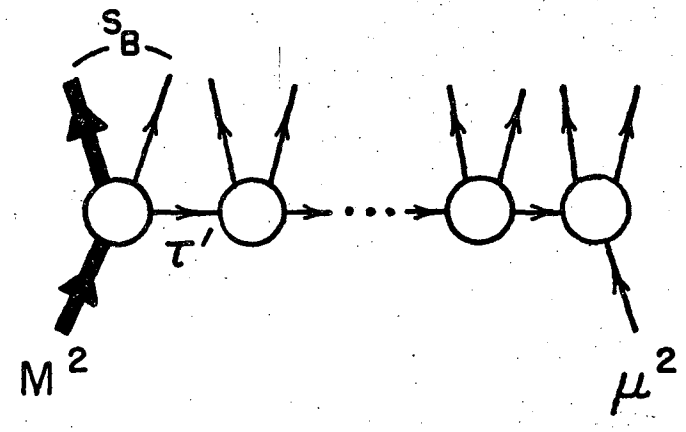

XBL728-3798

Fig. 9.

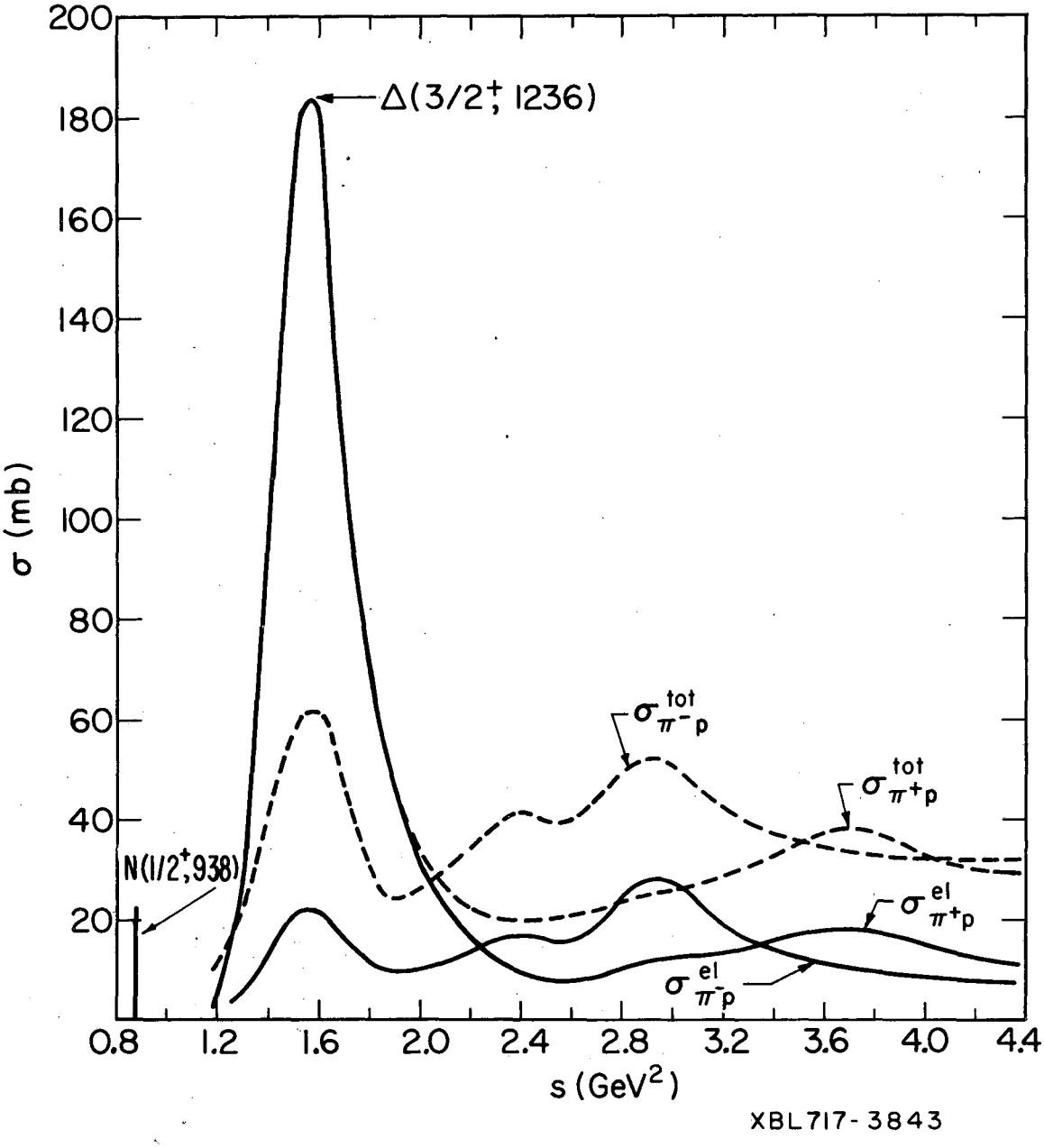
200
180
160
140
120
100
80
60
40
20
σ (mb)
Δ(3/2⁺; 1236)
N(1/2⁺;938)
$\sigma^{tot}_{\pi^- p}$
$\sigma^{tot}_{\pi^+ p}$
$\sigma^{el}_{\pi^+ p}$
$\sigma^{el}_{\pi^- p}$
0.8
1.2
1.6
2.0
2.4
2.8
3.2
3.6
4.0
4.4
s (GeV²)
XBL717-3843

Fig. 10.

XBL728-3799

Fig. 11.

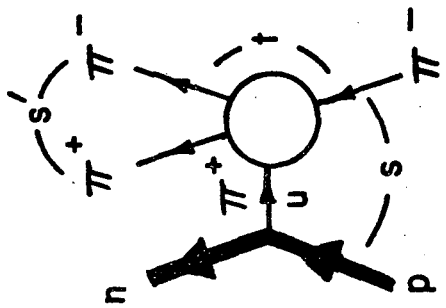

XBL728-3800

Fig. 12.

TECHNICAL INFORMATION DIVISION
LAWRENCE BERKELEY LABORATORY
UNIVERSITY OF CALIFORNIA
BERKELEY, CALIFORNIA 94720